Bralower, T.J., Premoli Silva, I., and Malone, M.J. (Eds.)
Proceedings of the Ocean Drilling Program, Scientific Results Volume 198

2. Cenozoic Calcareous Nannofossil Biostratigraphy, ODP Leg 198 Site 1208 (Shatsky Rise, Northwest Pacific Ocean)[1]

Paul R. Bown[2]

ABSTRACT

Ocean Drilling Program Site 1208 was drilled on the Central High of Shatsky Rise, and a highly expanded Neogene section (320 m), an extremely condensed Paleogene fragment (6.01 m), and a short Upper Cretaceous sequence (48.44 m) resting unconformably on Albian sediments were recovered. This paper presents the Cenozoic nannofossil biostratigraphy of Site 1208, focusing on the expanded Neogene section, comprising an apparently continuous middle Miocene–Holocene succession (Zones CN5–CN15), in which nannofloras are diverse and abundant throughout, and a fragmentary Paleogene–lower Miocene section (Zones CP8 to CN1c–CN2), which incorporates short fragments of the Paleocene/Eocene (Zones CP8–CP11) and Eocene/Oligocene (Zone CP16) boundary intervals bounded by three main unconformities. Two new species, *Sphenolithus arthurii* and *Fasciculithus fenestrellatus*, are described.

INTRODUCTION

Shatsky Rise is a moderately sized large igneous province that was erupted episodically at a hotspot triple junction intersection between 146 and 133 Ma (Tithonian–Valanginian) at equatorial latitudes (Bralower, Premoli Silva, Malone, et al., 2002). Site 1208 is located on the previously undrilled Central High (Fig. F1) at lower bathyal water

F1. Bathymetric map of Shatsky Rise, p. 14.

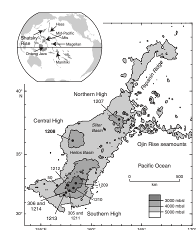

[1] Bown, P.R., 2005. Cenozoic calcareous nannofossil biostratigraphy, ODP Leg 198 Site 1208 (Shatsky Rise, northwest Pacific Ocean). *In* Bralower, T.J., Premoli Silva, I., and Malone, M.J. (Eds.), *Proc. ODP, Sci. Results,* 198, 1–44 [Online]. Available from World Wide Web: <http://www-odp.tamu.edu/publications/198_SR/VOLUME/CHAPTERS/104.PDF>. [Cited YYYY-MM-DD]

[2] Department of Earth Sciences, University College London, Gower Street, London WC1E 6BT, United Kingdom. Correspondence author: **p.bown@ucl.ac.uk**

Initial receipt: 22 February 2004
Acceptance: 23 March 2005
Web publication: 15 September 2005
Ms 198SR-104

depths (3346 m), and drilling was expected to penetrate 785 m of thick Neogene, Paleogene, and Upper Cretaceous units. However, coring at Site 1208 revealed a dramatically different sequence, notably a highly expanded Neogene section (320 m), an extremely condensed, incomplete, Paleogene fragment (6.01 m), and a short Upper Cretaceous sequence (48.44 m) resting unconformably on Albian sediments, where the hole was terminated due to drilling difficulties related to abundant chert (Bralower, Premoli Silva, Malone, et al., 2002).

This report presents the Cenozoic nannofossil biostratigraphy in the single hole cored at Site 1208. The expanded Neogene section comprises an apparently continuous middle Miocene–Holocene succession in which nannofloras are diverse and abundant throughout. Correlation with magnetostratigraphy is good and is presented in detail by Evans et al. (this volume). The Paleogene section is thin and condensed but incorporates short fragments of the Paleocene/Eocene and Eocene/Oligocene boundary intervals bounded by three main unconformities. Cretaceous nannofossil biostratigraphy is presented in Lees and Bown (this volume). The nannofossil biostratigraphy presented here gives greater detail than that in the Leg 198 *Initial Reports* volume (Bralower, Premoli Silva, Malone, et al., 2002) but does not differ significantly despite increased sampling resolution.

T1. Calcareous nannofossil stratigraphic range chart, Site 1208, p. 18.

T2. Paleogene–lower Miocene stratigraphic range chart, Site 1208, p. 19.

F2. Age-depth plot of Cretaceous calcareous nannofossil datums, Site 1208, p. 15.

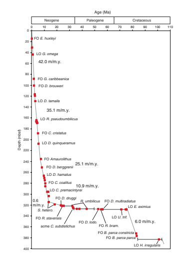

MATERIAL

Drilling at Site 1208 yielded the following succession: 252 m of cyclic upper Miocene–Holocene nannofossil ooze and nannofossil clay with significant amounts of diatoms throughout (5%–20%) (Subunit 1A of Bralower, Premoli Silva, Malone, et al., 2002); 60 m of dark orange-brown lower and middle Miocene claystone, nannofossil ooze, and chalk (Subunit 1B of Bralower, Premoli Silva, Malone, et al., 2002); 16 m of highly condensed lower Miocene–Paleocene claystone with phillipsite (zeolite) and manganese micronodules alternating with orange to yellow-brown nannofossil claystone and ooze (Subunit 1C of Bralower, Premoli Silva, Malone, et al., 2002); and 65 m of pure white Campanian nannofossil ooze and chalk (Unit 2 of Bralower, Premoli Silva, Malone, et al., 2002). The hole was terminated in Albian nannofossil chalk and chert.

F3. Age-depth plot of Neogene calcareous nannofossil datums, Site 1208, p. 16.

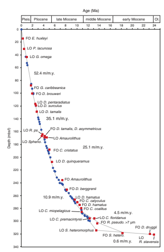

METHODS

Calcareous nannofossils were analyzed semiquantitatively using simple smear slides and standard light microscope techniques (Bown and Young, 1998); abundance and preservation categories are given in Table T1. Biostratigraphy is described with reference to the Cenozoic CP and CN zones of Okada and Bukry (1980). The timescale correlations are after Bralower, Premoli Silva, Malone, et al. (2002).

F4. Age-depth plot of Paleogene calcareous nannofossil datums, Site 1208, p. 17.

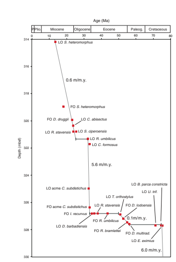

NANNOFOSSIL RESULTS

Nannofossil results are presented as stratigraphic range charts in Tables T1 and T2 and as age-depth plots in Figures F2, F3, and F4. The data used to create the age-depth plots are given in Table T3. Representative images of the nannofossil assemblages are given in Plates P1–P12

T3. Calcareous nannofossil datums, ages and depths, p. 20.

(Neogene: Pls. **P1, P2, P3, P4, P5, P6, P7;** Paleogene: Pls. **P8, P9, P10, P11, P12**). All cores were productive apart from a small number of samples from the dark brown claystones of the Paleocene–lower Miocene condensed interval (Subunit 1C). The middle Miocene–Holocene section yielded a beautiful succession of rich and abundant nannofossil assemblages. Preservation improved upsection but was also dependent upon which part of the sedimentary cycles had been sampled. The darker, diatom-rich intervals yielded more poorly preserved nannofossil assemblages. Diatoms are common in the smear slides from the middle Miocene–Holocene. The Paleogene condensed interval yielded extremely variable abundances, preservation, and diversity; 8 of 50 samples were barren, and evidence of mixing of assemblage components was observed. The Cretaceous samples yielded abundant, moderately preserved, and diverse assemblages.

NANNOFOSSIL BIOSTRATIGRAPHY

Miocene–Holocene

Neogene nannofossil biostratigraphy indicates a relatively complete stratigraphy with all zones from CN5 through CN15 (middle Miocene–Holocene) identified by their primary zonal fossils. Zones CN1–CN5 could not be easily distinguished because of the absence of the marker species *Sphenolithus belemnos*, *Helicosphaera ampliaperta*, and *Discoaster kugleri*. In addition, a number of CN subzones could not be recognized due to the absence of *D. kugleri* (Subzone CN5b), *Discoaster loeblichii*, *Discoaster neorectus* (Subzone CN8b), and *Amaurolithus amplificus* (subdivisions within Zone CN9) and an anomalously low last occurrence (LO) of *Triquetrorhabdulus rugosus* (Subzone CN10b). The absence of these zonal and subzonal markers is most likely due to rarity or ecological/biogeographic exclusion rather than significant missing time/sediment. The age-depth plot shows no obvious "benches" or datum event clusters that would indicate hiatuses, and the match with magnetostratigraphy is good (see Fig. **F3; Evans et al.,** this volume). Shipboard planktonic foraminifer biostratigraphy also indicated a relatively complete stratigraphy (Bralower, Premoli Silva, Malone, et al., 2002).

Miocene sediments older than Zone CN5 are more difficult to assign to biozones due to the absence, or rare and sporadic occurrence, of primary marker species, as listed above. *Sphenolithus heteromorphus*, although present, is sporadically distributed, and sphenoliths and *Helicosphaera* are generally rare throughout the Miocene section. A number of secondary lower–middle Miocene datum events are included on the age-depth plot (Fig. **F3**) (e.g., the LO of *Calcidiscus premacintyrei*, the LO of *Coccolithus miopelagicus*, and the LO of *Cyclicargolithus floridanus*), but there is no single solution that honors all the data points. Most likely, the LO of *S. heteromorphus* is anomalously low because of ecological exclusion of sphenoliths. This interpretation is supported by the presence of the Zone CN4 discoasters, *Discoaster muscicus* and *Discoaster petaliformis* (Young, 1998), in Sample 198-1208A-34X-5, 114 cm, and the first occurrence (FO) of large *Reticulofenestra pseudoumbilicus* (Young, 1998) in Sample 198-1208A-33X-5, 120 cm, which marks the top of Zone CN4.

P1. Helicosphaeraceae, Pontosphaeraceae, Noelaerhabdaceae, *Reticulofenestra*, p. 21.

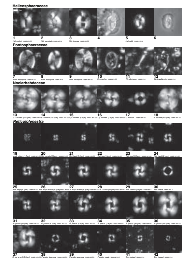

P2. *Gephyrocapsa,* Coccolithaceae, Calcidiscaceae, p. 23.

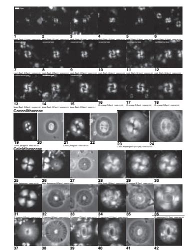

P3. Sphenolithaceae, Incertae sedis, Ceratolithaceae, p. 25.

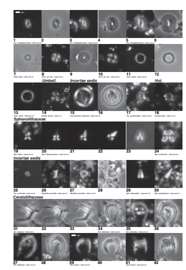

P4. *Triquetrorhabdulus,* Calcispheres, Discoasteraceae, p. 27.

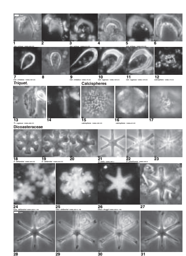

P5. Discoasteraceae II, p. 29.

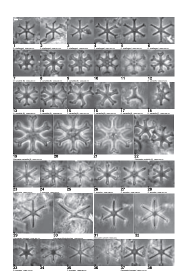

Paleocene–Lower Miocene

The lower Miocene–Paleocene section is a short (16 m), condensed section incorporating at least three major hiatuses (Figs. F2, F4). Nannofossil biostratigraphy is problematic in places due to mixing of stratigraphically incongruous assemblage components (Table T2). The mixing includes both upsection reworking and downsection bioturbation; the latter was prominent in this lithologic unit (Bralower, Premoli Silva, Malone, et al., 2002). Intriguingly, however, the unit appears to incorporate the Paleocene/Eocene boundary and the Eocene/Oligocene boundary carbonate pulse (e.g., Bralower, Premoli Silva, Malone, et al., 2002; Lyle, Wilson, Janecek, et al., 2002).

The upper Oligocene–lower Miocene section (~1.1 m) is characterized by low-diversity assemblages dominated by *Discoaster deflandrei* and *C. floridanus*. The FOs of *Sphenolithus ciperoensis* and *Discoaster druggii;* LOs of *Reticulofenestra bisecta, S. ciperoensis*, and *Cyclicargolithus abisectus;* and occurrence of *Triquetrorhabdulus carinatus* allow the identification of the subzones/intervals CP19–CN1a, CN1a, and CN1c–CN2.

The uppermost Eocene–lower Oligocene section (~5.5 m) can be assigned to Zone CP16 based on the absence of Eocene discoasters (e.g., *Discoaster barbadiensis*) and the presence of *Isthmolithus recurvus* and *Reticulofenestra umbilicus*. Subzones CP16a–CP16c can be identified using the first common occurrence of *Clausicoccus subdistichus* (Subzone CP16b) and the LO of *Coccolithus formosus* (Subzone CP16c). The base of Subzone CP16b is marked in the core by a prominent switch from dark brown, in places barren, claystones to lighter-colored, grayish orange nannofossil ooze (see fig. F15 in Chapter 4, Shipboard Scientific Party, 2002). This switch to carbonate accumulation may reflect a significant post-Eocene/Oligocene boundary deepening of the carbonate compensation depth (CCD) and is an event that is recognized elsewhere in the Pacific (van Andel, 1975; e.g., DSDP Sites 42, 70, 161, 162, and ODP Site 1217; Lyle, Wilson, Janecek, et al. 2002). This uppermost Eocene–lower Oligocene section is bounded top and bottom by hiatuses comprising Zones CP17–CP18 (lower Oligocene) and Zones CP12–CP15 (middle–upper Eocene), respectively.

The short (~0.75 m) upper Paleocene–lower Eocene section (see fig. F17 in Chapter 4, Shipboard Scientific Party, 2002) can be correlated with Zones CP8–CP11, based on the ranges of *Discoaster multiradiatus*, *Discoaster diastypus*, *Rhomboaster bramlettei, Tribrachiatus orthostylus*, and *Discoaster lodoensis* and the decline and LO of *Fasciculithus* (Bralower et al., 1995; Aubry et al., 1996; Schmitz et al., 1997; see also Bralower, Premoli Silva, Malone, et al., 2002). The increase in *Zygrhablithus bijugatus,* recorded at this level elsewhere on Shatsky Rise, was not seen at Site 1208 because this species was absent throughout. Its absence may be due to greater dissolution at this deeper site.

A number of the samples in this interval yielded mixed assemblages but consideration of range continuity, abundance, and overall assemblage character allowed construction of a relatively coherent stratigraphy (Fig. F3). Nevertheless, the following zonal designations should be viewed with some caution. Zone CP8 is identified using the FO of *D. multiradiatus* and Subzone CP9a the FOs of *D. diastypus* and *R. bramlettei*. Subzone CP9b is identified using the LO of *Tribrachiatus contortus*, although this taxon was extremely rare; however, further support is provided by the additional FOs of *T. orthostylus* (although problematic due to mixing) and *Sphenolithus radians*. Zone CP10 is recognized using

P6. Discoasteraceae III, p. 31.

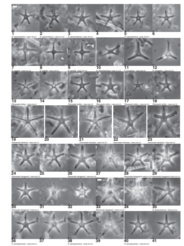

P7. Discoasteraceae IV, Diatoms, p. 33.

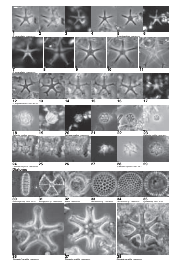

P8. Noelaerhabdaceae, Coccolithaceae, p. 35.

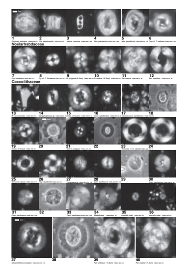

P9. Sphenolithaceae, p. 37.

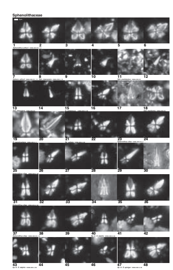

P10. Discoasteraceae V, p. 39.

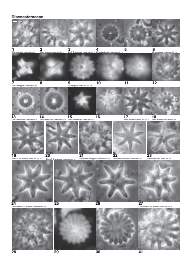

the FO of *D. lodoensis*, and the LO of *T. orthostylus,* at the top of this interval, indicates the presence of Zone CP11. The FO of *Toweius crassus* is a problematic datum and was not identified at this site. The Paleocene–Eocene section lies unconformably on Upper Cretaceous sediments. Cretaceous biostratigraphy is presented in detail in Lees and Bown (this volume).

SUMMARY

The expanded Neogene section comprises a continuous middle Miocene–Holocene section incorporating Zones CN4–CN15 and yielding rich nannofossil and diatom assemblages. A number of subzone intervals were not recognized because of missing marker taxa. *Sphenolithus* and *Helicosphaera* exhibit particularly sporadic distribution patterns, but this is thought to be due to taxic exclusion or rarity rather than significant missing stratigraphy.

The lower Miocene–Paleocene section is a short (16 m), condensed section incorporating at least three major hiatuses. Intriguingly, the unit appears to incorporate the Paleocene/Eocene boundary and the Eocene/Oligocene boundary carbonate pulse.

The upper Oligocene–lower Miocene section (Zones CP19–CN2) (~1.1 m) is characterized by low-diversity assemblages dominated by *D. deflandrei* and *C. floridanus*.

The uppermost Eocene–lower Oligocene section (~5.5 m) includes the *C. subdistichus* acme Subzone CP16a, which is marked in the core by a prominent switch from dark brown claystones to lighter-colored grayish orange nannofossil ooze. This switch to carbonate accumulation is a significant post-Eocene/Oligocene event that is recognized elsewhere in the Pacific.

The short (~0.75 m) upper Paleocene–lower Eocene section appears to represent a short, continuous stratigraphic fragment that can be correlated with Zones CP8–CP11, based on the ranges of *D. multiradiatus*, *D. diastypus*, *R. bramlettei, T. orthostylus*, and *D. lodoensis* and the decline and LO of *Fasciculithus*. The Paleocene/Eocene Thermal Maximum level lies within this interval.

ACKNOWLEDGMENTS

This research used samples provided by the Ocean Drilling Program (ODP). ODP is funded by the U.S. National Science Foundation (NSF) and participating countries under management of the Joint Oceanographic Institutions (JOI), Inc. Funding for ODP participation was provided by the The Natural Environment Research Council (NERC), UK. The author would also like to acknowledge the contributions made by the other ODP Leg 198 shipboard palaeontologists, namely, Mark Leckie, Maria Rose Petrizzo, Jason Eleson, Isabella Premoli Silva, Tim Bralower, and Kotaro Takeda, and the science party in general, who made the leg so productive and enjoyable.

P11. *Rhomboaster, Tribrachiatus,* p. 41.

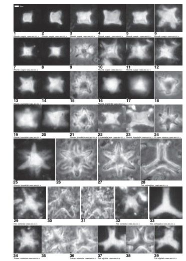

P12. Fasciculithaceae, p. 43.

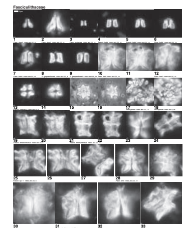

REFERENCES

Aubry, M.-P., Berggren, W.A., Stott, L., and Sinha, A., 1996. The upper Paleocene–lower Eocene stratigraphic record and the Paleocene/Eocene boundary carbon isotope excursion: implications for geochronology. *In* Knox, R.W.O'B., Corfield, R.M., and Dunay, R.E. (Eds.), *Correlation of the Early Paleogene in Northwestern Europe.* Geol. Soc. Spec. Publ., 101:353–380.

Bown, P.R. (Ed.), 1998. *Calcareous Nannofossil Biostratigraphy:* Dordrecht, The Netherlands (Kluwer Academic Publ.).

Bown, P.R., 2005. Palaeogene calcareous nannofossils from the Kilwa and Lindi areas of coastal Tanzania (Tanzania Drilling Project sites 2003–4). *J. Nannoplankton Res.,* 27:21–95.

Bown, P.R., and Young, J.R., 1998. Techniques. *In* Bown, P.R. (Ed.), *Calcareous Nannofossil Biostratigraphy:* Dordrecht, The Netherlands (Kluwer Academic Publ.), 16–28.

Bralower, T.J., 1987. Valanginian to Aptian calcareous nannofossil stratigraphy and correlation with the upper M-sequence magnetic anomalies. *Mar. Micropaleontol.,* 11:293–310.

Bralower, T.J., Premoli Silva, I., Malone, M.J., et al., 2002. *Proc. ODP, Init. Repts.,* 198 [CD-ROM]. Available from: Ocean Drilling Program, Texas A&M University, College Station TX 77845-9547, USA.

Bralower, T.J., Sliter, W.V., Arthur, M.A., Leckie, R.M., Allard, D.J., and Schlanger, S.O., 1993. Dysoxic/anoxic episodes in the Aptian–Albian (Early Cretaceous). *In* Pringle, M.S., Sager, W.W., Sliter, W.V., and Stein, S. (Eds.), *The Mesozoic Pacific: Geology, Tectonics, and Volcanism.* Geophys. Monogr., 77:5–37.

Bralower, T.J., Zachos, J.C., Thomas, E., Parrow, M., Paull, C.K., Kelly, D.C., Premoli Silva, I., Sliter, W.V., and Lohmann, K.C., 1995. Late Paleocene to Eocene paleoceanography of the equatorial Pacific Ocean: stable isotopes recorded at Ocean Drilling Program Site 865, Allison Guyot. *Paleoceanography,* 10:841–865.

Burnett, J.A., with contributions from Gallagher, L.T., and Hampton, M.J., 1998. Upper Cretaceous. *In* Bown, P.R. (Ed.), *Calcareous Nannofossil Biostratigraphy:* Dordrecht, The Netherlands (Kluwer Academic Publ.), 132–199.

Klaus, A., and Sager, W.W., 2002. Data report: High-resolution site survey seismic reflection data for ODP Leg 198 drilling on Shatsky Rise, northwest Pacific. *In* Bralower, T.J., Premoli Silva, I., Malone, M.J., et al., *Proc. ODP, Init. Repts.,* 198 [Online]. Available from World Wide Web: http://www-odp.tamu.edu/publications/198_IR/chap_11/chap_11.htm.

Lyle, M., Wilson, P.A., Janecek, T.R., et al., 2002. *Proc. ODP, Init. Repts.,* 199 [CD-ROM]. Available from: Ocean Drilling Program, Texas A&M University, College Station TX 77845-9547, USA.

Okada, H., and Bukry, D., 1980. Supplementary modification and introduction of code numbers to the low-latitude coccolith biostratigraphic zonation (Bukry, 1973; 1975). *Mar. Micropaleontol.,* 5:321–325.

Perch-Nielsen, K., 1985a. Cenozoic calcareous nannofossils. *In* Bolli, H.M., Saunders, J.B., and Perch-Nielsen, K. (Eds.), *Plankton Stratigraphy:* Cambridge (Cambridge Univ. Press), 427–554.

Perch-Nielsen, K., 1985b. Mesozoic calcareous nannofossils. *In* Bolli, H.M., Saunders, J.B., and Perch-Nielsen, K. (Eds.), *Plankton Stratigraphy:* Cambridge (Cambridge Univ. Press), 329–426.

Robinson, S.A., Williams, T., and Bown, P.R., 2004. Fluctuations in biosiliceous production and the generation of Early Cretaceous oceanic anoxic events in the Pacific Ocean (Shatsky Rise, ODP Leg 198). *Paleoceanography,* 19(PA4024):10.1029/2004PA001010.

Roth, P.H., 1978. Cretaceous nannoplankton biostratigraphy and oceanography of the northwestern Atlantic Ocean. *In* Benson, W.E., Sheridan, R.E., et al., *Init. Repts. DSDP,* 44: Washington (U.S. Govt. Printing Office), 731–759.

Roth, P.H., 1983. Jurassic and Lower Cretaceous calcareous nannofossils in the western North Atlantic (Site 534): biostratigraphy, preservation, and some observations on biogeography and paleoceanography. *In* Sheridan, R.E., Gradstein, F.M., et al., *Init. Repts. DSDP,* 76: Washington (U.S. Govt. Printing Office), 587–621.

Schmitz, B., Asaro, F., Molina, E., Monechi, S., von Salis, K., and Speuijer, R.P., 1997. High-resolution iridium $\delta^{13}C$, $\delta^{18}O$, foraminifera and nannofossil profiles across the latest Paleocene benthic extinction event at Zumaya, Spain. *Palaeogeogr., Palaeoclimatol., Palaeoecol.,* 133:49–68.

van Andel, T.H., 1975. Mesozoic/Cenozoic calcite compensation depth and the global distribution of calcareous sediments. *Earth Planet. Sci. Lett.,* 26:187–194.

Young, J.R., 1998. Neogene. In Bown, P.R. (Ed.), Calcareous Nannofossil Biostratigraphy: Dordrecht, The Netherlands (Kluwer Academic Publ.), 225–265.

Young, J.R., Bergen, J.A., Bown, P.R., Burnett, J.A., Fiorentino, A., Jordan, R.W., Kleijne, A., van Niel, B.E., Ton Romein, A.J., von Salis, K., 1997. Guidelines for coccolith and calcareous nannofossil terminology. Paleontology, 40:875–912.

Young, J.R., and Bown, P.R., 1997. Cenozoic calcareous nannoplankton classification. *J. Nannoplankton Res.,* 19:36–47.

APPENDIX A

Systematic Taxonomy

The systematic paleontology section includes brief taxonomic notes on a number of key taxa and the description of two new species, *Sphenolithus arthurii* and *Fasciculithus fenestrellatus*. The taxonomy follows the classification and organization of Young and Bown (1997) and Young (1998). Only bibliographic references not included in Perch-Nielsen (1985a, 1985b) and Bown (1998) are included in the reference list. A full taxonomic list of species cited in this paper follows in "Appendix B," p. 10. Descriptive terminology follows the guidelines of Young et al. (1997), and the following abbreviations are used in taxonomic descriptions: LM = light microscope, XPL = cross polarized light, PC = phase-contrast illumination. The taxa are illustrated in Plates P1–P12.

Neocrepidolithus grandiculus Bown, 2005
Pl. P8, figs. 4, 5

Description: Large murolith coccolith with a broad rim, unicyclic in XPL, and a narrow, vacant central area. The central area width is variable, usually around the same width as the rim, but may be narrower or closed. Similar in morphology to the Jurassic species *Crepidolithus crassus* and distinguished from other Paleogene *Neocrepidolithus* species by its larger size, open central area, and simple unicyclic rim image.

Dimensions: length = 9.0–13.5 µm; width = 6.5–10.0 µm.

Occurrence: lower Eocene (Zone CP9) at Site 1208; Zone CP8–Subzone CP9b, Tanzania (Bown, 2005).

Discoaster cf. *D. araneus* Bukry, 1971
Pl. P10, figs. 2, 19, 20, 24–27

Remarks: Large discoasters with 6–8 rays, free for around half their length, and curving, although the degree of curvature is variable. Arrangement of rays usually shows asymmetry. The central area is broad and appears to be flat and unadorned.

Differentiation: Does not possess a central area stem like *D. araneus* and differentiated from *D. lodoensis* by asymmetry, variable degree of ray curvature, and shorter free ray length.

Occurrence: upper Paleocene–lower Eocene (Zone CP8–Subzone CP9b) at Site 1208.

Sphenolithus villae Bown, 2005
Pl. P9, figs. 23–39

Description: Large, robust sphenolith with tall proximal cycle (lower quadrants in XPL; see Young et al., 1997) and tall, tapering, monocrystalline apical spine. The base is taller than it is wide and appears as four quadrants separated by a clear extinction cross at 0°; the lower quadrants are as much as twice as tall as the upper quadrants. At 45° the base is crossed by diagonal extinction lines, and lateral cycles are visible, showing varying birefringence. The spine is tall (usually equivalent to the height of the base, but may be shorter) and inserted into the upper quadrants in a V-shape. The spine appears to be monocrystalline and is dark at 0° and brightest at 45°. Comparable in general morphology to the Miocene *Sphenolithus belemnos;* however, *S. villae* is larger and more robustly constructed, with blockier spine and base.

Dimensions: height = 9.0–12.0 µm; width = 3.0–5.0 µm.

Occurrence: lower Eocene (Zone CP9) at Site 1208; Subzones CP8b–CP9b, Tanzania (Bown, 2005)

Sphenolithus arthurii sp. nov.
Pl. P9, figs. 1–7

Derivation of name: Named for Mike Arthur, paleoceanographer and ODP 198 shipboard scientist.

Diagnosis: Large, robust sphenolith with squat, square base and short, sharply tapering spine. The base is coarsely constructed, square-shaped, and crossed by an extinction cross at 0°; the lower and upper quadrants are near equidimensional. At 45° the base is crossed by diagonal extinction lines. The spine is short (equal to or shorter than the base) and tapers sharply to a point. The spine is compound and may be divided by a median extinction line at 0°, where it is darkest but still visible. The spine is brightest at 45°.

Differentiation: Comparable in general morphology to *Sphenolithus radians*; however, *S. arthurii* is larger and more coarsely constructed, with blockier spine and base.

Dimensions: height = 7.0–11.0 µm; width = 5.0–8.0 µm.

Holotype: Pl. P9, fig. 3 (fig. 4 is the same specimen).

Paratype: Pl. P9, fig. 5 (fig. 6 is the same specimen); Pl. P9, fig. 2 (fig. 1 is the same specimen).

Type locality: Leg 198, Site 1208, Shatsky Rise, northwest Pacific Ocean.

Type level: lower Eocene, Sample 198-1208A-36X-CC, 1.5 cm (Subzone CP9b).

Occurrence: lower Eocene (Subzone CP9b) at Site 1208.

Fasciculithus fenestrellatus sp. nov.
Pl. P12, figs. 19–24

Derivation of name: From *fenestra*, *ella*, and *atus*, meaning "with little windows," and referring to the distinct ornamentation of this fasciculith.

Diagnosis: Large, tall fasciculith that tapers toward its base and is ornamented with large, rectangular fenestrae delineated by distinct longitudinal and transverse ridges. The fasciculith is taller than it is wide. The LM image is not the typical two blocks seen in smaller fasciculiths, the median extinction line being indistinct.

Dimensions: height = 12.3 µm; width = 9.8 µm.

Holotype: Pl. P12, fig. 21 (figs. 21–24 are the same specimen).

Paratype: Pl. P12, fig. 19 (fig. 20 is the same specimen).

Type locality: Leg 198, Site 1208, Shatsky Rise, northwest Pacific Ocean.

Type level: upper Paleocene, Sample 198-1208A-36X-CC, 12 cm (Zone CP8).

Occurrence: upper Paleocene (Zone CP8) at Site 1208.

Fasciculithus sp. 1
Pl. P12, figs. 25–27

Description: Large fasciculith that tapers slightly toward its base and is ornamented with thick, rounded, protruding ridges. This fasciculith is broader than it is tall and possesses a relatively wide central opening. The LM image is not the typical two blocks seen in smaller fasciculiths.

Dimensions: height = 11.0 µm; width = 14.4 µm.

Occurrence: upper Paleocene (Zone CP8) at Site 1208.

Rhomboaster cuspis Bramlette and Sullivan, 1961
Pl. P11, figs. 1–12

Remarks: Broadly cubic-rhombic morphology with variable-length ray extensions from the corners. Cubic shape prevents the nannolith lying on one corner, as seen in *Rhomboaster bramlettei*.

Rhomboaster bramlettei (Bronnimann and Stradner, 1960) Bybell and Self-Trail, 1995
Pl. P11, figs. 13–27

Remarks: LM image shows two offset, superimposed, triradiate structures; rarely observed in side view (Pl. P11, figs. 22, 23).

APPENDIX B

Taxonomic List

A full list of all taxa cited in the text, figures, and range charts is given below. Most bibliographic references can be found in Perch-Nielsen (1985a, 1985b) and Bown (1998).

Amaurolithus amplificus (Bukry and Percival, 1971) Gartner and Bukry, 1975
Amaurolithus bizarrus (Bukry, 1973) Gartner and Bukry, 1975
Amaurolithus delicatus Gartner and Bukry, 1975
Amaurolithus primus (Bukry and Percival, 1971) Gartner and Bukry, 1975
Amaurolithus tricorniculatus (Gartner, 1967) Gartner and Bukry, 1975
Bramletteius serraculoides Gartner, 1969
Broinsonia parca (Stradner, 1963) Bukry, 1969 ssp. *constricta* Hattner et al., 1980
Broinsonia parca (Stradner, 1963) Bukry, 1969 ssp. *parca*
Calcidiscus leptoporus (Murray and Blackman, 1898) Loeblich and Tappan, 1978
Calcidiscus macintyrei (Bukry and Bramlette, 1969) Loeblich and Tappan, 1978
Calcidiscus pacificanus (Bukry, 1971) Varol, 1989
Calcidiscus premacintyrei Theodoridis, 1984
Calcidiscus tropicus Kamptner, 1956 sensu Gartner, 1992
Calciosolenia Gran, 1912
Calciosolenia murrayi Gran, 1912
Catinaster calyculus Martini and Bramlette, 1963
Catinaster coalitus Martini and Bramlette, 1963
Catinaster coalitus Martini and Bramlette, 1963 ssp. *extensus* Peleo-Alampay, Bukry, Liu, and Young, 1998
Ceratolithoides aculeus (Stradner, 1961) Prins and Sissingh in Sissingh, 1977
Ceratolithus cristatus Kamptner, 1950
Ceratolithus rugosus Bukry and Bramlette, 1968
Ceratolithus telesmus Norris, 1965
Chiasmolithus Hay, Mohler, and Wade, 1966
Chiasmolithus consuetus (Bramlette and Sullivan, 1961) Hay and Mohler, 1967
Chiasmolithus eograndis Perch-Nielsen, 1971
Chiasmolithus grandis (Bramlette and Riedel, 1964) Radomski, 1968
Chiasmolithus nitidus Perch-Nielsen, 1971
Chiasmolithus solitus (Bramlette and Sullivan, 1961) Locker, 1968
Chiphragmalithus barbatus Perch-Nielsen, 1967
Clausicoccus subdistichus (Roth and Hay in Hay et al., 1967) Prins, 1979
Coccolithus eopelagicus (Bramlette and Riedel, 1954) Bramlette and Sullivan, 1961
Coccolithus formosus (Kamptner, 1963) Wise, 1973
Coccolithus miopelagicus Bukry, 1971
Coccolithus pelagicus (Wallich, 1871) Schiller, 1930
Coronocyclus nitescens (Kamptner, 1963) Bramlette and Wilcoxon, 1967
Crepidolithus crassus (Deflandre in Deflandre and Fert, 1954) Noël, 1965
Cretarhabdus Bramlette and Martini, 1964
Cruciplacolithus edwardsii Romein, 1979
Cryptococcolithus mediaperforatus (Varol, 1991) de Kaenel and Villa, 1996
Cyclicargolithus abisectus (Müller, 1970) Wise, 1973
Cyclicargolithus floridanus (Roth and Hay in Hay et al., 1967) Bukry, 1971
Discoaster anartios Bybell and Self-Trail, 1995
Discoaster araneus Bukry, 1971
Discoaster asymmetricus Gartner, 1969
Discoaster barbadiensis Tan, 1927
Discoaster bellus Bukry and Percival, 1971
Discoaster bergenii Knuttel et al., 1989
Discoaster berggrenii Bukry, 1971b
Discoaster binodosus Martini, 1958
Discoaster blackstockiae Bukry, 1973

Discoaster bollii Martini and Bramlette, 1963
Discoaster braarudii Bukry, 1971
Discoaster brouweri Tan, 1927, emend. Bramlette and Riedel, 1954
Discoaster calcaris Gartner, 1967
Discoaster challengeri Bramlette and Riedel, 1954
Discoaster deflandrei Bramlette and Riedel, 1954
Discoaster diastypus Bramlette and Sullivan, 1961
Discoaster druggii Bramlette and Wilcoxon, 1967
Discoaster elegans Bramlette and Sullivan, 1961
Discoaster exilis Martini and Bramlette, 1963
Discoaster falcatus Bramlette and Sullivan, 1961
Discoaster hamatus Martini and Bramlette, 1963
Discoaster kuepperi Stradner, 1959
Discoaster kugleri Martini and Bramlette, 1963
Discoaster lenticularis Bramlette and Sullivan, 1961
Discoaster lodoensis Bramlette and Riedel, 1954
Discoaster loeblichii Bukry, 1971
Discoaster mahmoudii Perch-Nielsen, 1981
Discoaster mediosus Bramlette and Sullivan, 1961
Discoaster megastypus (Bramlette and Sullivan, 1961) Perch-Nielsen, 1985
Discoaster mohleri Bukry and Percival, 1971
Discoaster musicus Stradner, 1959
Discoaster nobilis Martini, 1961
Discoaster neorectus Bukry, 1971
Discoaster pentaradiatus Tan, 1927
Discoaster petaliformis Moshkovitz and Ehrlich, 1980
Discoaster prepentaradiatus Bukry and Percival, 1971
Discoaster quinqueramus Gartner, 1969
Discoaster salisburgensis Stradner, 1961
Discoaster surculus Martini and Bramlette, 1963
Discoaster tamalis Kamptner, 1967
Discoaster tanii Bramlette and Riedel, 1954
Discoaster tanii Bramlette and Riedel, 1954, ssp. *nodifer* Bramlette and Riedel, 1954
Discoaster tanii Bramlette and Riedel, 1954, ssp. *ornatus* Bramlette and Wilcoxon, 1967
Discoaster triradiatus Tan, 1927
Discoaster variabilis Martini and Bramlette, 1963
Eiffellithus eximius (Stover, 1966) Perch-Nielsen, 1968
Ellipsolithus macellus (Bramlette and Sullivan, 1961) Sullivan, 1964
Emiliania huxleyi (Lohmann, 1902) Hay and Mohler in Hay et al., 1967
Ericsonia robusta (Bramlette and Sullivan, 1961) Perch-Nielsen, 1977
Fasciculithus alanii Perch-Nielsen, 1971
Fasciculithus aubertae Haq and Aubry, 1981
Fasciculithus bobii Perch-Nielsen, 1971
Fasciculithus clinatus Bukry, 1971
Fasciculithus fenestrellatus sp. nov.
Fasciculithus schaubii Hay and Mohler in Hay et al., 1967
Fasciculithus sidereus Bybell and Self-Trail, 1995
Fasciculithus tonii Perch-Nielsen, 1971
Fasciculithus tympaniformis Hay and Mohler in Hay et al., 1967
Florisphaera profunda Okada and Honjo, 1973
Gephyrocapsa Kamptner, 1943
Gephyrocapsa aperta Kamptner, 1963
Gephyrocapsa caribbeanica Boudreaux and Hay, 1967
Gephyrocapsa oceanica Kamptner, 1943
Gephyrocapsa omega Bukry, 1973
Gephyrocapsa parallela Hay and Beaudry, 1973
Girgisia gammation (Bramlette and Sullivan, 1961) Varol, 1989
Hayella situliformis Gartner, 1969

Hayesites irregularis (Thierstein in Roth and Thierstein, 1972) Applegate et al. in Covington and Wise, 1987
Helicosphaera ampliaperta Bramlette and Wilcoxon, 1967
Helicosphaera carteri (Wallich, 1877) Kamptner, 1954
Helicosphaera granulata (Bukry and Percival, 1971) Jafar and Martini, 1975
Helicosphaera inversa (Gartner, 1980) Theodoridis, 1984
Helicosphaera sellii (Bukry and Bramlette, 1969) Jafar and Martini, 1975
Helicosphaera wallichii (Lohmann, 1902) Boudreaux and Hay, 1969
Hughesius gizoensis Varol, 1989
Isthmolithus recurvus Deflandre in Deflandre and Fert, 1954
Markalius inversus (Deflandre in Deflandre and Fert, 1954) Bramlette and Martini, 1964
Micula murus (Martini, 1961) Bukry, 1973
Minylitha convallis Bukry, 1973
Neocrepidolithus Romein, 1979
Neocrepidolithus grandiculus Bown, 2005
Neosphaera coccolithomorpha Lecal-Schlauder, 1950
Pontosphaera discopora Schiller, 1925
Pontosphaera japonica (Takayama, 1967) Nishida, 1971
Pontosphaera multipora (Kamptner, 1948) Roth, 1970
Pseudoemiliania lacunosa (Kamptner, 1963) Gartner, 1969
Pseudoemiliania ovata (Bukry, 1973) Young, 1998
Reticulofenestra asanoi Sato and Takayama, 1992
Reticulofenestra dictyoda (Deflandre in Deflandre and Fert, 1954) Stradner in Stradner and Edwards, 1968
Reticulofenestra haqii Backman, 1978
Reticulofenestra lockeri Müller, 1970
Reticulofenestra minuta Roth, 1970
Reticulofenestra minutula (Gartner, 1967) Haq and Berggren, 1978
Reticulofenestra pseudoumbilicus (Gartner, 1967) Gartner, 1969
Reticulofenestra rotaria Theodoridis, 1984
Reticulofenestra scrippsae (Bukry and Percival, 1971) Roth, 197
Reticulofenestra stavensis (Levin and Joerger, 1967) Varol, 1989
Reticulofenestra umbilicus (Levin, 1965) Martini and Ritzkowski, 1968
Rhabdosphaera clavigera Murray and Blackman, 1898
Rhomboaster cuspis Bramlette and Sullivan, 1961
Rhomboaster bramlettei (Bronnimann and Stradner, 1960) Bybell and Self-Trail, 1995
Rhomboaster spineus (Shafik and Stradner, 1961) Perch-Nielsen, 1984
Sphenolithus abies Deflandre in Deflandre and Fert, 1954
Sphenolithus arthurii sp. nov.
Sphenolithus belemnos Bramlette and Wilcoxon, 1967
Sphenolithus calyculus Bukry, 1985
Sphenolithus capricornutus Bukry and Percival, 1971
Sphenolithus ciperoensis Bramlette and Wilcoxon, 1967
Sphenolithus conspicuus Martini, 1976
Sphenolithus delphix Bukry, 1973
Sphenolithus dissimilis Bukry and Percival, 1971
Sphenolithus editus Perch-Nielsen in Perch-Nielsen et al., 1978
Sphenolithus heteromorphus Deflandre, 1953
Sphenolithus intercalaris Martini, 1976
Sphenolithus moriformis (Brönnimann and Stradner, 1960) Bramlette and Wilcoxon, 1967
Sphenolithus predistentus Bramlette and Wilcoxon, 1967
Sphenolithus radians Deflandre in Grassé, 1952
Sphenolithus spiniger Bukry, 1971
Sphenolithus pseudoradians Bramlette and Wilcoxon, 1967
Sphenolithus villae Bown, 2005
Syracosphaera pulchra Lohmann, 1902
Tetralithoides symeonidesii Theodoridis, 1984
Toweius Hay and Mohler, 1967

Toweius callosus Perch-Nielsen, 1971
Toweius pertusus (Sullivan, 1965) Romein, 1979
Tranolithus orionatus (Reinhardt, 1966) Reinhardt, 1966
Tribrachiatus contortus (Stradner, 1958) Bukry, 1972
Tribrachiatus digitalis Aubry, 1995
Tribrachiatus orthostylus Shamrai, 1963
Triquetrorhabdulus carinatus Martini, 1965
Triquetrorhabdulus rugosus Bramlette and Wilcoxon, 1967
Umbellosphaera tenuis (Kamptner, 1937) Paasche in Markali and Paasche, 1955
Umbilicosphaera hulburtiana Gaarder, 1970
Umbilicosphaera jafari Müller, 1974
Umbilicosphaera rotula (Kamptner, 1956) Varol, 1982
Umbilicosphaera sibogae (Weber-van Bosse, 1901) Gaarder, 1970
Uniplanarius trifidus (Stradner in Stradner and Papp, 1961) Hattner and Wise, 1980

Figure F1. Bathymetric map of Shatsky Rise and the location of Shatsky Rise in the Pacific Ocean (inset). The main map indicates the location of ODP and DSDP sites on Shatsky Rise, whereas the inset shows the location of Shatsky Rise in the Pacific Ocean relative to other Cretaceous volcanic features (modified from Bralower, Premoli Silva, Malone, et al., 2002; Klaus and Sager, 2002; Robinson et al., 2004).

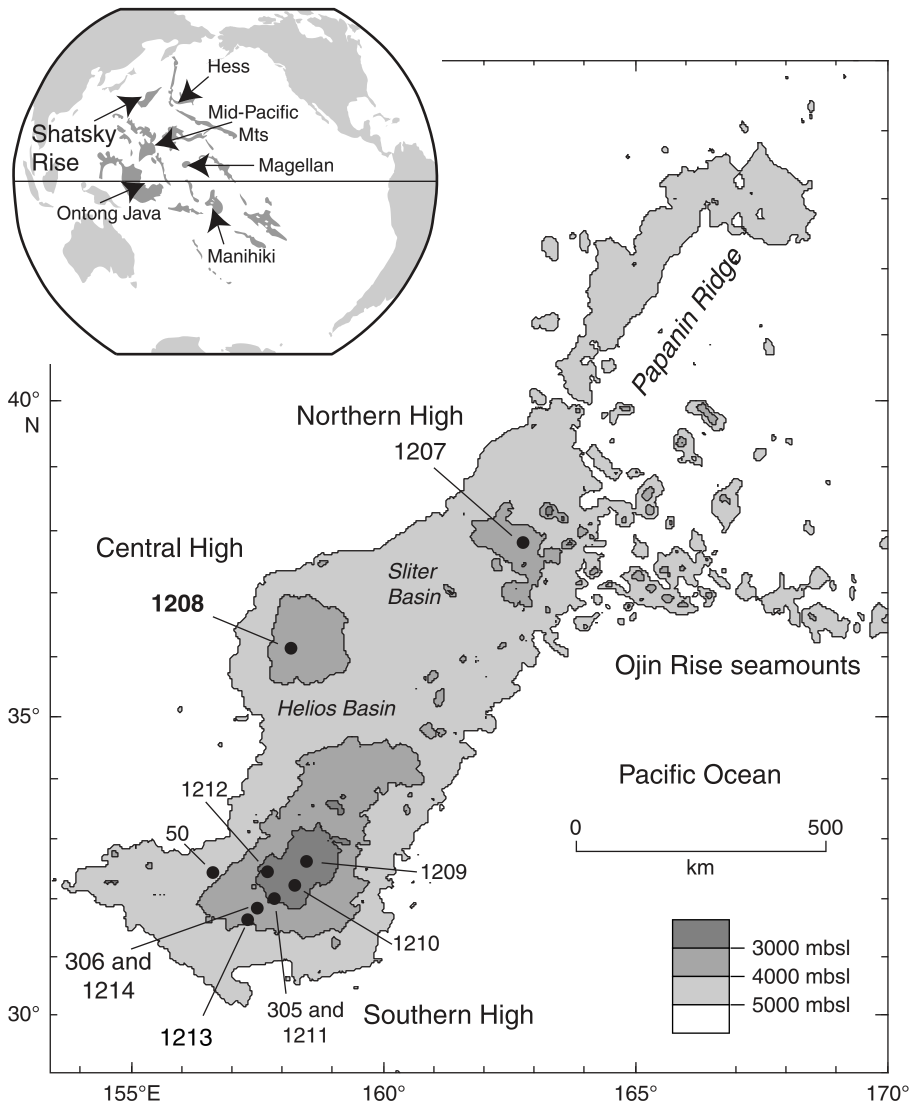

Figure F2. Age-depth plot of calcareous nannofossil datums (red squares) from Site 1208. Cretaceous data from this work and Lees and Bown (this volume). FO = first occurrence, LO = last occurrence.

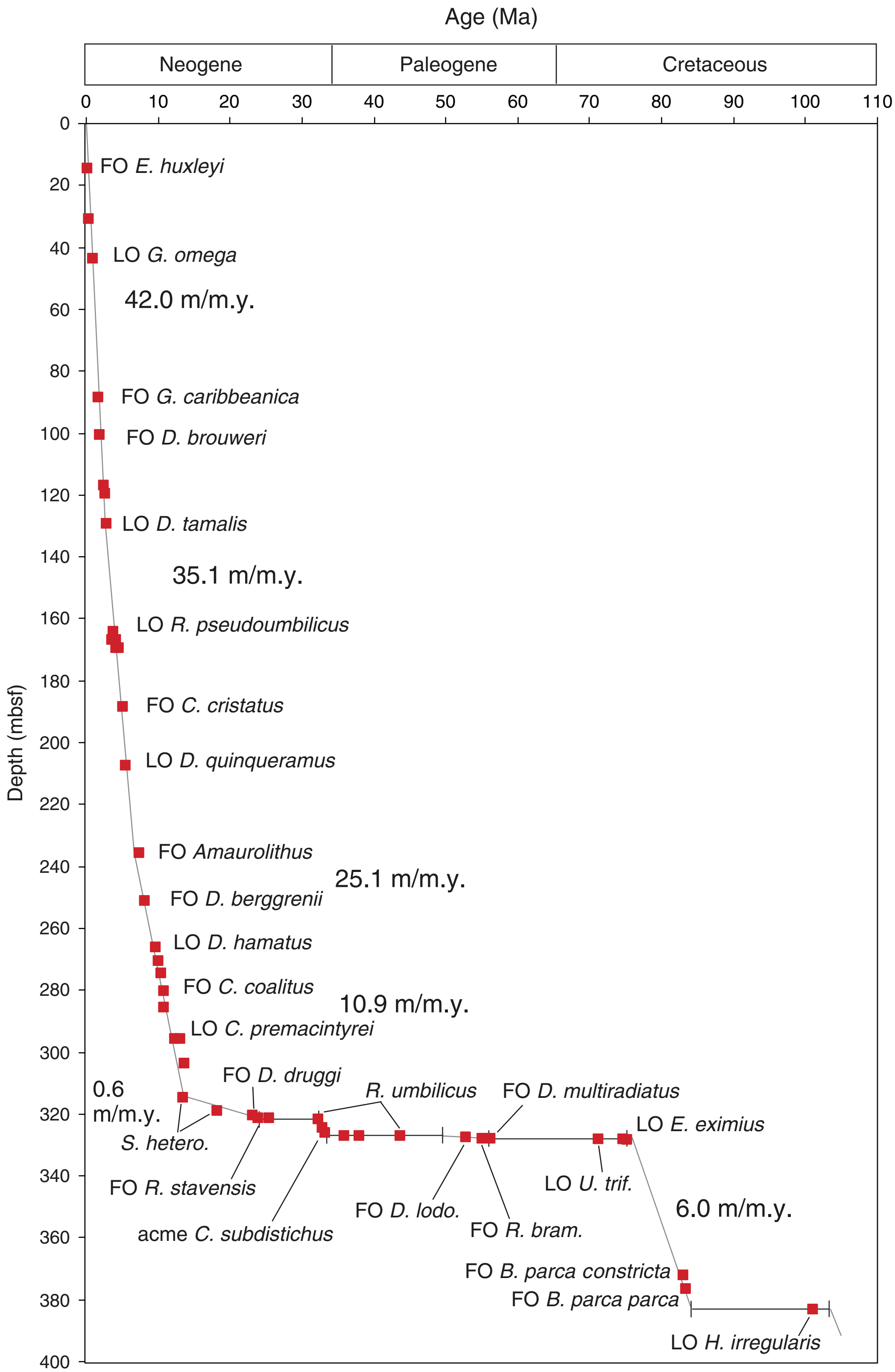

Figure F3. Age-depth plot of calcareous nannofossil datums (red squares) for the Neogene of Site 1208. Magnetostratigraphic datums from Evans et al. (this volume) (blue circles). FO = first occurrence, LO = last occurrence.

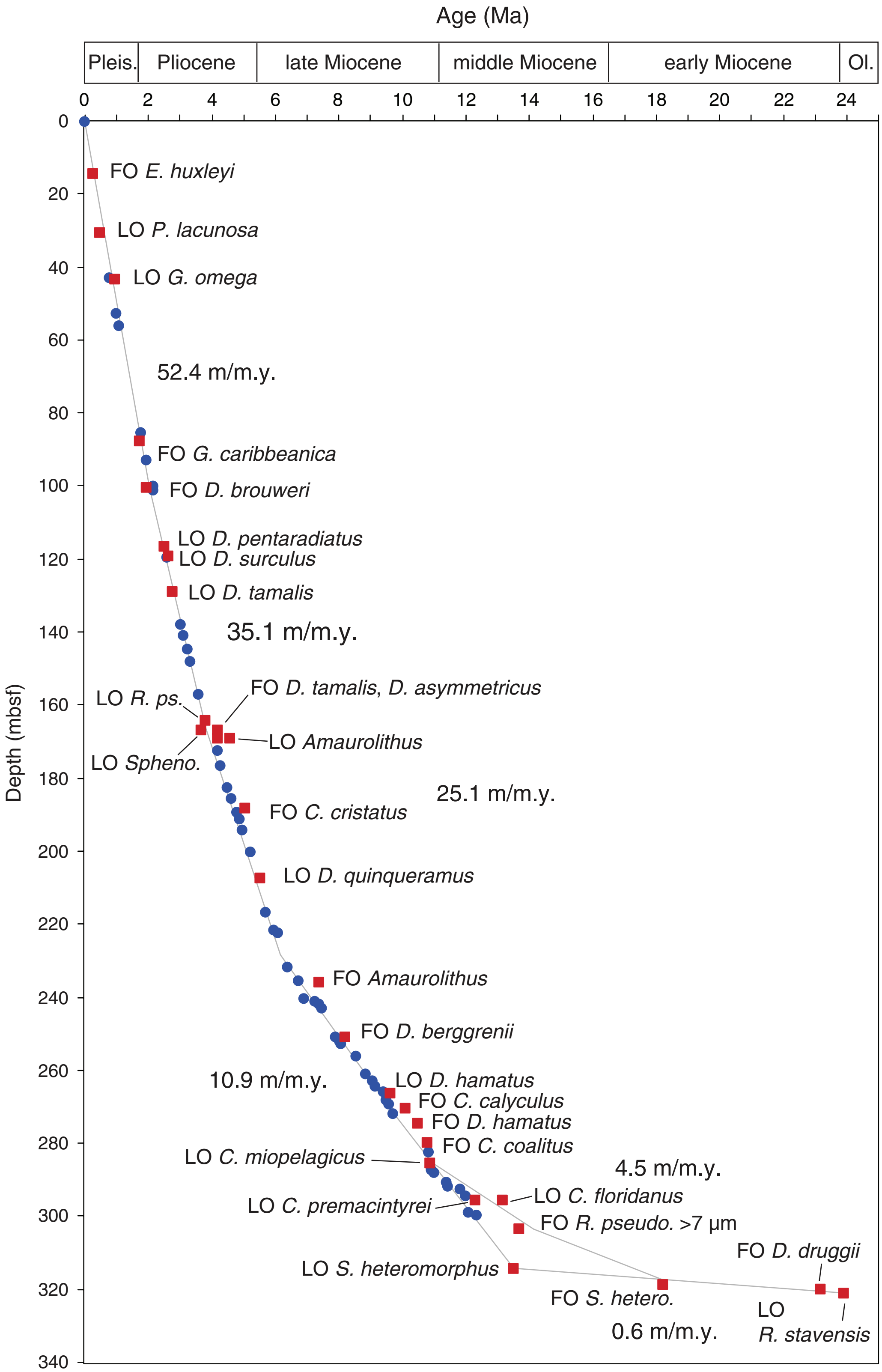

Figure F4. Age-depth plot of calcareous nannofossil datums (red squares) for the Paleogene of Site 1208. Cretaceous data from this work and Lees and Bown (this volume). FO = first occurrence, LO = last occurrence.

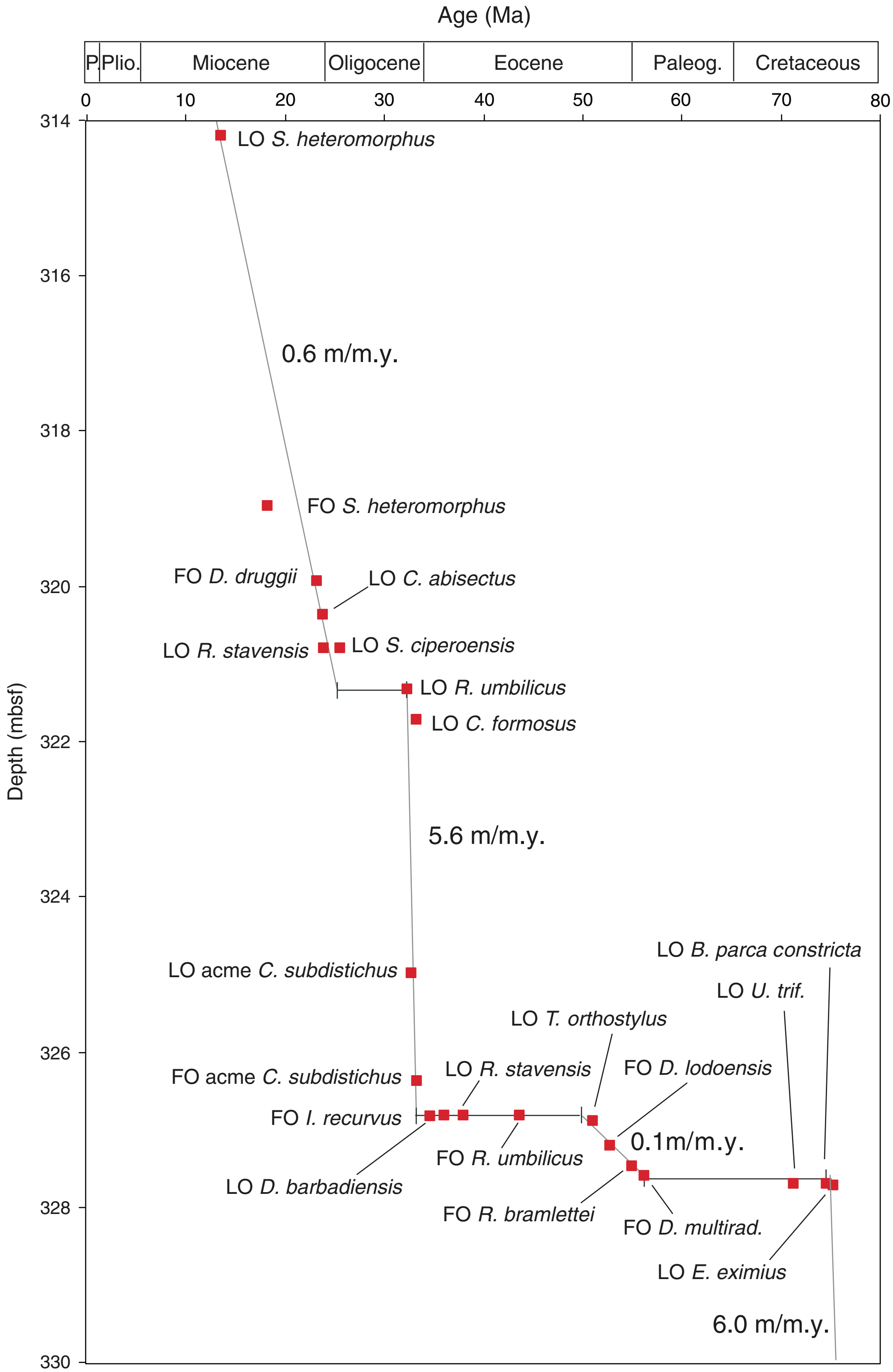

Table T1. Calcareous nannofossil stratigraphic range chart, Site 1208. (This table is available in an **oversized format**.)

Table T2. Paleogene–lower Miocene stratigraphic range chart, Site 1208. (This table is available in an **oversized format.**)

Table T3. Calcareous nannofossil datums, ages and depths.

Datum	Depth (mbsf)	Age (Ma)	Age data source
FO *Emiliania huxleyi*	14.24	0.26	Shipboard Scientific Party, 2002a
LO *P. lacunosa*	30.30	0.46	Shipboard Scientific Party, 2002a
FO *G. omega*	43.11	0.95	Shipboard Scientific Party, 2002a
FO *G. caribbeanica*	87.90	1.73	Shipboard Scientific Party, 2002a
LO *D. brouweri*	100.16	1.95	Shipboard Scientific Party, 2002a
LO *D. pentaradiatus*	116.40	2.52	Shipboard Scientific Party, 2002a
LO *D. surculus*	119.08	2.63	Shipboard Scientific Party, 2002a
LO *D. tamalis*	128.70	2.78	Shipboard Scientific Party, 2002a
LO Large *Reticulofenestra*	163.90	3.82	Shipboard Scientific Party, 2002a
FO *D. tamalis*	166.66	4.20	Young, 1998
LO *Sphenolithus*	166.66	3.65	Shipboard Scientific Party, 2002a
LO *Amaurolithus*	168.88	4.56	Shipboard Scientific Party, 2002a
FO *D. asymmetricus*	168.88	4.20	Young, 1998
FO *C. cristatus*	187.90	5.07	Shipboard Scientific Party, 2002a
LO *D. quinqueramus*	207.00	5.54	Shipboard Scientific Party, 2002a
FO *Amaurolithus*	235.52	7.39	Shipboard Scientific Party, 2002a
FO *D. quinqueramus*	250.80	8.20	Shipboard Scientific Party, 2002a
FO *D. berggrenii*	250.80	8.20	Shipboard Scientific Party, 2002a
FO *D. hamatus*	265.94	9.63	Shipboard Scientific Party, 2002a
FO *C. calyculus*	270.10	10.10	Young, 1998
FO *D. hamatus*	274.20	10.48	Shipboard Scientific Party, 2002a
FO *C. coalitus*	279.70	10.79	Shipboard Scientific Party, 2002a
LO *C. miopelagicus*	285.06	10.90	Young, 1998
LO *C. premacintyrei*	295.41	12.30	Young, 1998
LO *C. floridanus*	295.41	13.19	Shipboard Scientific Party, 2002a
FO *R. pseudoumbilicus* (>7 µm)	303.10	13.70	Young, 1998
LO *S. heteromorphus*	314.17	13.52	Shipboard Scientific Party, 2002a
FO *S. heteromorphus*	319.05	18.20	Shipboard Scientific Party, 2002a
FO *D. druggii*	319.92	23.20	Shipboard Scientific Party, 2002a
LO *C. abisectus*	320.30	23.50	Young, 1998
LO *R. bisecta*	320.79	23.90	Shipboard Scientific Party, 2002a
LO *S. ciperoensis*	320.79	25.50	Shipboard Scientific Party, 2002a
LO *R. umbilicus*	321.30	32.30	Shipboard Scientific Party, 2002a
LO *C. formosus*	321.75	32.80	Shipboard Scientific Party, 2002a
Top acme *C. subdistichus*	325.00	32.80	Young, 1998
Base acme *C. subdistichus*	326.30	33.30	Shipboard Scientific Party, 2002a
FO *I. recurvus*	326.80	36.00	Shipboard Scientific Party, 2002a
FO *R. stavensis*	326.80	38.00	Shipboard Scientific Party, 2002a
FO *R. umbilicus*	326.80	43.70	Shipboard Scientific Party, 2002a
LO *D. barbadiensis*	326.82	34.30	Shipboard Scientific Party, 2002a
LO *T. orthostylus*	326.83	50.60	Shipboard Scientific Party, 2002a
FO *D. lodoensis*	327.20	52.80	Shipboard Scientific Party, 2002a
FO *Rhomboaster*	327.48	55.00	Shipboard Scientific Party, 2002a
FO *D. multiradiatus*	327.58	56.20	Shipboard Scientific Party, 2002a
LO *U. trifidus*	327.68	71.30	Shipboard Scientific Party, 2002a
LO *B. parca constricta*	327.68	74.60	Shipboard Scientific Party, 2002a
LO *E. eximius*	327.70	75.30	Shipboard Scientific Party, 2002a
FO *B. parca constricta*	371.53	82.50	Shipboard Scientific Party, 2002a
FO *B. parca parca*	376.14	83.40	Shipboard Scientific Party, 2002a
LO *H. irregularis*	382.90	101.00	Shipboard Scientific Party, 2002a

Notes: Age data from Shipboard Scientific Party (2002; Chapter 2, figs. F4, F5; and references therein) and Young (1998). Cretaceous data from this work and **Lees and Bown** (this volume).

Plate P1. Helicosphaeraceae, Pontosphaeraceae, Noelaerhabdaceae, *Reticulofenestra*. Taxonomic organization and concepts are generally comparable to those of Young and Bown (1997) and Young (1998). Images with black background are cross-polarized light images; those with light backgrounds are phase-contrast images. **1.** *Helicosphaera carteri* (Sample 198-1208A-8H-CC). **2.** *Helicosphaera granulata* (Section 198-1208A-34X-5). **3, 4.** *Helicosphaera inversa* (Sample 198-1208A-3H-CC). **5, 6.** *Helicosphaera sellii* (Section 198-1208A-13H-5). **7, 8.** *Pontosphaera discopora;* (7) Sample 198-1208A-9H-CC, (8) Section 198-1208A-2H-5. **9.** *Pontosphaera multipora* (Sample 198-1208A-18H-CC). **10.** *Syracosphaera pulchra* (Sample 198-1208A-8H-CC). **11.** *Rhabdosphaera clavigera* (Section 198-1208A-1H-4). **12.** *Calciosolenia brasiliensis* (Section 198-1208A-1H-4). **13.** *Cyclicargolithus ?abisectus* (11.4 µm) (Sample 198-1208A-32X-CC). **14–17.** *Cyclicargolithus floridanus;* (14) 10.1 µm (Sample 198-1208A-27X-CC), (15) 9.3 µm (Sample 198-1208A-32X-CC), (16) 7.5 µm (Sample 198-1208A-32X-CC), (17) Sample 198-1208A-35X-CC. **18.** *Reticulofenestra bisecta* (10.6 µm) (Sample 198-1208A-35X-CC). **19.** Small reticulofenestrids (~1.7 µm) (Sample 198-1208A-18H-CC). **20.** *Reticulofenestra minuta* (2.8 µm) (Sample 198-1208A-5H-CC). **21–25.** *Reticulofenestra haqii;* (21) 3.1 µm (Sample 198-1208A-18H-CC), (22) 4 µm (Sample 198-1208A-27X-CC), (23) 4.3 µm (Sample 198-1208A-16H-CC), (24) 4.1 µm (Sample 198-1208A-14H-CC), (25) 4.7 µm (Sample 198-1208A-9H-CC). **26, 27.** *Reticulofenestra haqii-asanoi;* (26) 5.4 µm (Core 198-1208A-7H), (27) 6.3 µm (Sample 198-1208A-6H). **28, 29.** *Reticulofenestra asanoi;* (28) 6.6 µm (Sample 198-1208A-6H-CC), (29) 6.8 µm (Section 198-1208A-6H-5). **30.** *Reticulofenestra rotaria* (Section 198-1208A-25X-4). **31–37.** *Reticulofenestra pseudoumbilicus;* (31) 5.0 µm (Sample 198-1208A-27X-CC), (32) 6.1 µm (Sample 198-1208A-26X-CC), (33) 6.9 µm (Sample 198-1208A-26X-CC), (34) 7.8 µm (Sample 198-1208A-19H-CC), (36) 11.5 µm (Sample 198-1208A-28X-CC), (37) 9.2 µm with grill (Sample 198-1208A-18H-CC). **38, 39.** *Pseudoemiliania lacunosa;* (38) Sample 198-1208A-16H-CC, (39) Sample 198-1208A-4H-CC. **40.** *Pseudoemiliania ovata* (Sample 198-1208A-9H-CC). **41, 42.** *Emiliania huxleyi* (Section 198-1208A-1H-4). (**Plate shown on next page.**)

Plate P1 (continued). (Caption shown on previous page.)

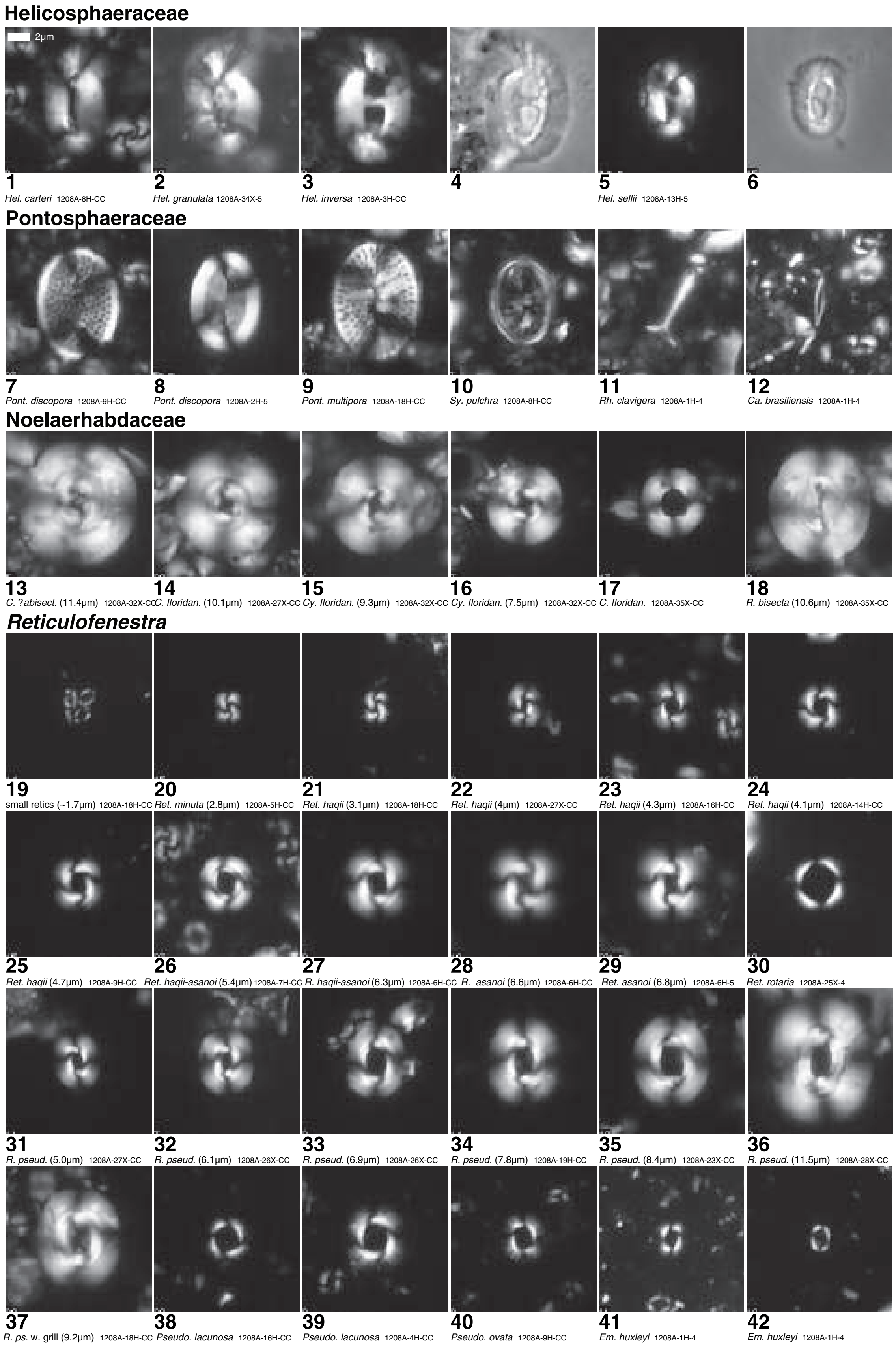

Plate P2. *Gephyrocapsa,* Coccolithaceae, Calcidiscaceae. Taxonomic organization and concepts are generally comparable to those of Young and Bown (1997) and Young (1998). Images with black background are cross-polarized light images; those with light backgrounds are phase-contrast images. **1–6.** *Gephyrocapsa* (small); (1) 1.4 µm (Sample 198-1208A-2H-CC), (2) 2.1 µm (Sample 198-1208A-9H-CC), (3) 2.1 µm (Sample 198-1208A-18H-CC), (4) 2.8 µm (Sample 198-1208A-5H-CC), (5) 2.9 µm (Sample 198-1208A-4H-CC), (6) 2.9 µm (Sample 198-1208A-3H-CC). **7–12.** *Gephyrocapsa* (medium); (7–10) *G. oceanica,* (7) 3.8 µm (Sample 198-1208A-4H-CC), (8) 3.8 µm (Sample 198-1208A-2H-CC), (9) 3.8 µm (Sample 198-1208A-1H-CC), (10) 4.4 µm (Sample 198-1208A-2H-CC), (11, 12) *G. caribbeanica,* (11) 4.1 µm (Sample 198-1208A-8H-CC), (12) 4.3 µm (Sample 198-1208A-8H-CC). **13–15.** *Gephyrocapsa* (large); (13) *G. caribbeanica,* 5.0 µm (Sample 198-1208A-8H-CC), (14, 15) *G. oceanica,* (14) 5.1 µm (Sample 198-1208A-8H-CC), (15) 5.6 µm (Sample 198-1208A-1H-1). **16–18.** *Gephyrocapsa omega;* (16) 5.2 µm (Sample 198-1208A-1H-CC), (17) 5.0 µm (Sample 198-1208A-5H-CC), (18) 5.3 µm (Sample 198-1208A-4H-CC). **19–22.** *Coccolithus pelagicus;* (19, 20) Sample 198-1208A-30X-CC, (21, 22) Sample 198-1208A-19H-CC. **23, 24.** *Coccolithus miopelagicus* (15.1 µm) (Sample 198-1208A-31X-CC). **25–28.** *Calcidiscus leptoporus;* (25) Sample 198-1208A-14H-CC, (26, 27) 6.3 µm (Sample 198-1208A-27X-CC), (28) 8.8 µm (Sample 198-1208A-24X-CC). **29–33.** *Calcidiscus tropicus;* (29, 30) 8.7 µm (Sample 198-1208A-13H-CC), (31) 8.8 µm (Sample 198-1208A-21X-CC), (32) 8.9 µm (Sample 198-1208A-32X-CC), (33) 7.8 µm (Sample 198-1208A-18H-CC). **34–38.** *Calcidiscus macintyrei;* (34, 35) 11.2 µm (Sample 198-1208A-32X-CC), (36) 11.7 µm (Sample 198-1208A-26X-CC), (37, 38) 11.2 µm (Sample 198-1208A-24X-CC). **39–42.** *Calcidiscus premacintyrei;* (39) Sample 198-1208A-33X-CC, (40, 41) 11.2 µm (Sample 198-1208A-32X-CC), (42) 11.5 µm (Sample 198-1208A-31X-CC). (**Plate shown on next page.**)

Plate P2 (continued). (Caption shown on previous page.)

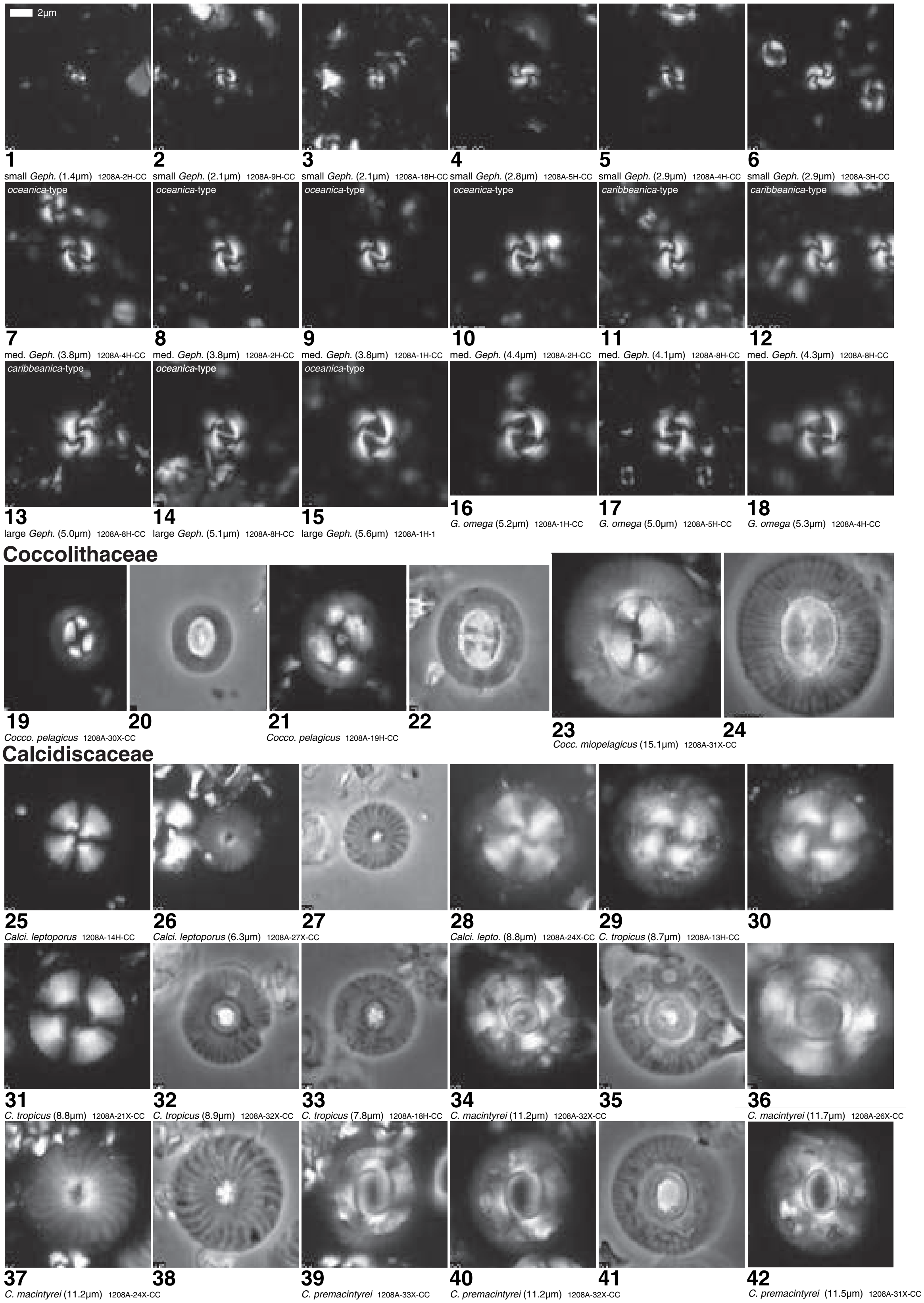

Plate P3. Sphenolithaceae, *Incertae sedis,* Ceratolithaceae. Taxonomic organization and concepts are generally comparable to those of Young and Bown (1997) and Young (1998). Images with black background are cross-polarized light images; those with light backgrounds are phase-contrast images. **1–6.** *Cryptococcolithus mediaperforatus;* (1, 2) Sample 198-1208A-24X-CC, (3, 4) Sample 198-1208A-33X-CC, (5, 6) Sample 198-1208A-32X-CC. **7.** *Umbilicosphaera jafari* (Sample 198-1208A-18H-CC). **8–10.** *Umbilicosphaera sibogae sibogae;* (8, 9) Sample 198-1208A-5H-CC, (10) Sample 198-1208A-2H-CC. **11–13.** *Umbilicosphaera rotula;* (11, 12) Sample 198-1208A-27X-CC, (13) Sample 198-1208A-30X-CC. **14.** *Umbellosphaera tenuis* (Sample 198-1208A-1H-1). **15, 16.** *Coronocyclus nitescens* (Sample 198-1208A-33X-CC). **17.** *Tetralithoides symeonidesii* (Sample 198-1208A-14H-CC). **18.** Holococcolith (Sample 198-1208A-1H-CC). **19.** *Sphenolithus abies* (Sample 198-1208A-25X-CC). **20–23.** *Sphenolithus heteromorphus* (Sample 198-1208A-33X-CC). **24.** *Sphenolithus moriformis* (Sample 198-1208A-35X-CC). **25.** *Florisphaera profunda* (Sample 198-1208A-7H-CC). **26–28.** *Minylitha convallis;* (26) Sample 198-1208A-28X-CC, (27, 28) Sample 198-1208A-27X-CC. **29.** *Sphenolithus intercalaris* (Sample 198-1208A-35X-CC). **30.** *Sphenolithus predistentus* (Sample 198-1208A-35X-CC). **31–33.** *Amaurolithus bizarrus* (Sample 198-1208A-22X-5). **34–38.** *Amaurolithus delicatus;* (34) Sample 198-1208A-23X-CC, (35, 36) Sample 198-1208A-24X-CC, (37, 38) Sample 198-1208A-19H-CC. **39–42.** *Amaurolithus primus;* (39, 40) Sample 198-1208A-25X-CC, (41, 42) Sample 198-1208A-26X-CC. (**Plate shown on next page.**)

Plate P3 (continued). (Caption shown on previous page.)

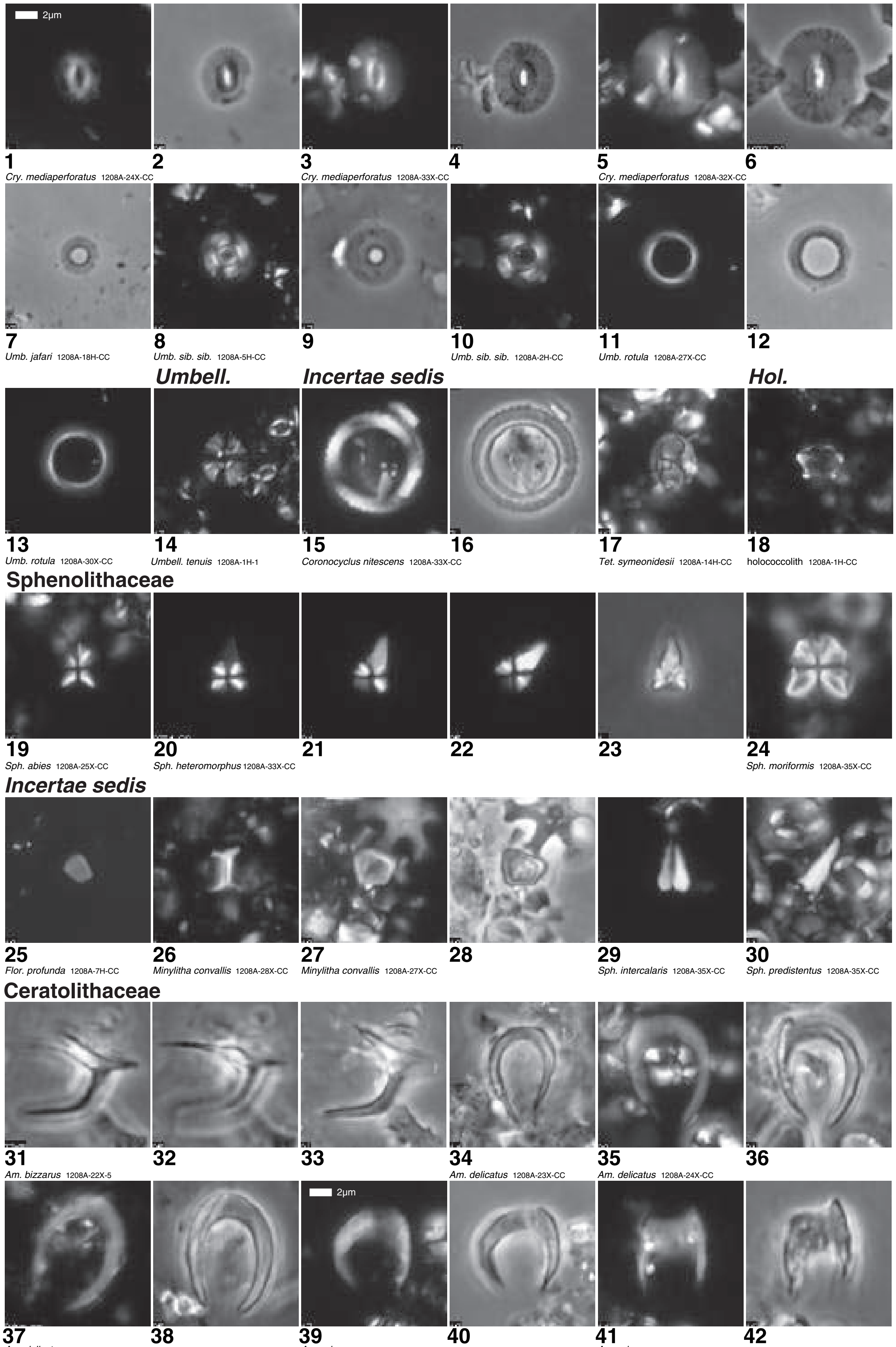

Plate P4. *Triquetrorhabdulus,* Calcispheres, Discoasteraceae. Taxonomic organization and concepts are generally comparable to those of Young and Bown (1997) and Young (1998). Images with black background are cross-polarized light images; those with light backgrounds are phase-contrast images. **1–6.** *Amaurolithus primus;* (1, 2) Sample 198-1208A-26X-CC, (3, 4) Sample 198-1208A-21X-CC, (5, 6) Sample 198-1208A-24X-CC. **7–9.** *Ceratolithus cristatus;* (7, 8) Sample 198-1208A-19H-CC, (9) Sample 198-1208A-1H-CC. **10, 11.** *Ceratolithus rugosus;* (10) Sample 198-1208A-19H-CC, (11) Sample 198-1208A-14H-CC. **12, 15–17.** Calcisphere (12) Sample 198-1208A-1H-CC, (15) Sample 198-1208A-18H-CC, (16, 17) Sample 198-1208A-4H-CC. **13, 14.** *Triquetrorhabdulus rugosus* (Sample 198-1208A-28X-CC). **18–20, 24, 25.** *Discoaster deflandrei;* (18) Sample 198-1208A-32X-CC, (19, 20) Sample 198-1208A-34X-CC, (24, 25) Sample 198-1208A-35X-3, 149 cm. **21.** *Discoaster exilis* (Sample 198-1208A-30X-4). **22, 23.** *Discoaster petaliformis* (Sample 198-1208A-34X-5). **26, 27.** *Discoaster druggii* (Sample 198-1208A-35X-3, 149 cm). **28–31.** *Discoaster exilis* (Sample 198-1208A-32X-CC). (**Plate shown on next page.**)

Plate P4 (continued). (Caption shown on previous page.)

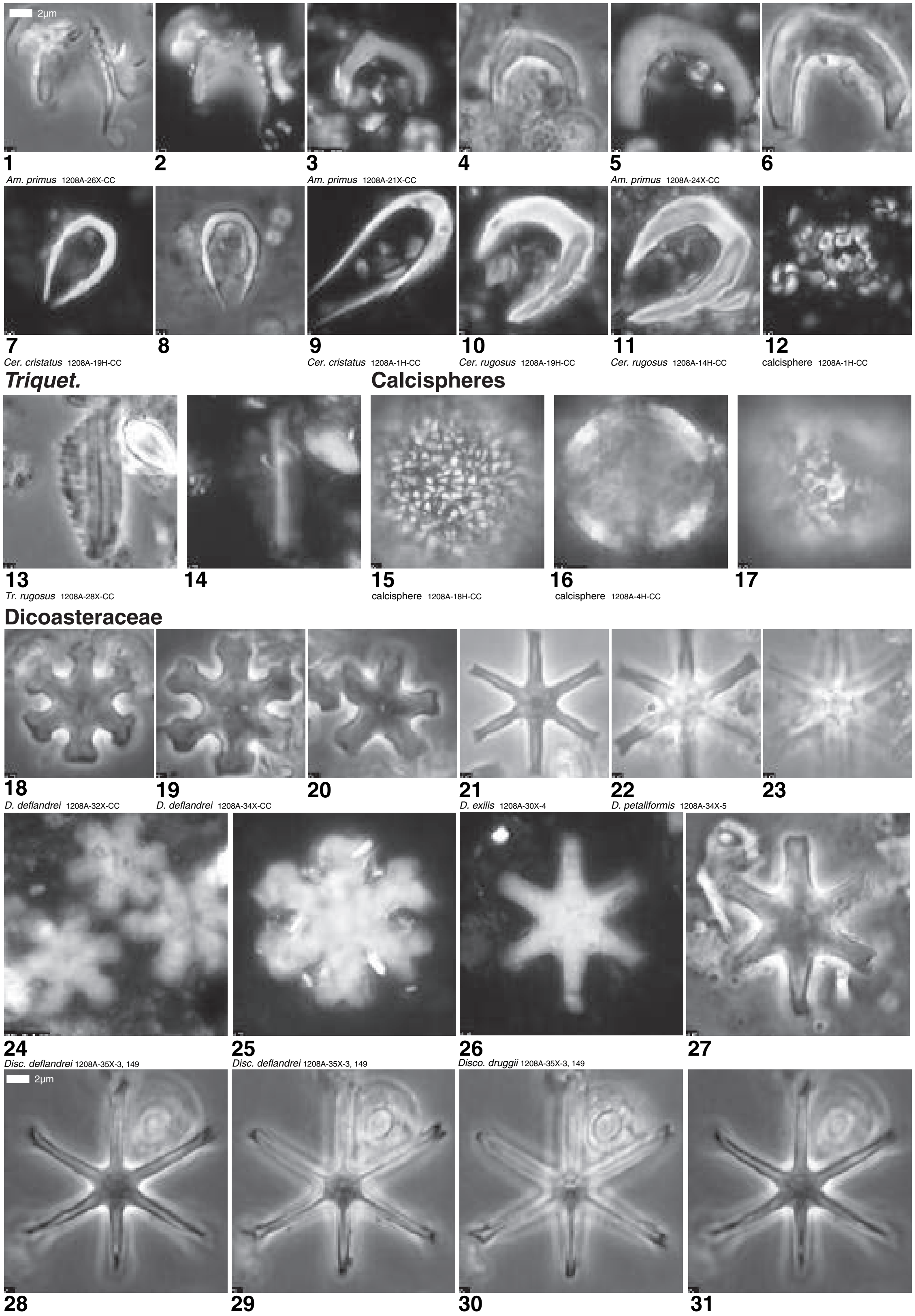

Plate P5. Discoasteraceae II. Taxonomic organization and concepts are generally comparable to those of Young and Bown (1997) and Young (1998). Images with black background are cross-polarized light images; those with light backgrounds are phase-contrast images. **1–6.** *Discoaster challengeri;* (1, 5) Sample 198-1208A-30X-CC, (2, 3) Sample 198-1208A-27X-CC, (4) Sample 198-1208A-33X-CC, (6) Sample 198-1208A-23X-CC. **7–22.** *Discoaster variabilis;* (7–11, 13, 14) 6 (Sample 198-1208A-28X-CC), (12) Sample 198-1208A-27X-CC, (15) 5 (Sample 198-1208A-25X-CC), (16) 5 (Sample 198-1208A-29X-CC), (17) 3 (Sample 198-1208A-26X-CC), (18) 7 (Sample 198-1208A-29X-CC), (19–21) 6 (Sample 198-1208A-25X-CC), (22) 6 (Sample 198-1208A-29X-CC). **23–28.** *Discoaster surculus;* (23) Sample 198-1208A-14H-CC, (24, 25) Sample 198-1208A-13H-CC, (26) Sample 198-1208A-18H-CC, (27) Sample 198-1208A-19H-CC, (28) Sample 198-1208A-21X-CC. **29, 33–38.** *Discoaster brouweri;* (29) Sample 198-1208A-28X-CC, (33, 34) Sample 198-1208A-17H-CC, (35, 36) Sample 198-1208A-18H-CC, (37, 38) Sample 198-1208A-27X-CC. **30.** *Discoaster blackstockiae* (Sample 198-1208A-24X-CC). **31, 32.** *Discoaster calcaris* (Sample 198-1208A-29X-2). (**Plate shown on next page.**)

Plate P5 (continued). (Caption shown on previous page.)

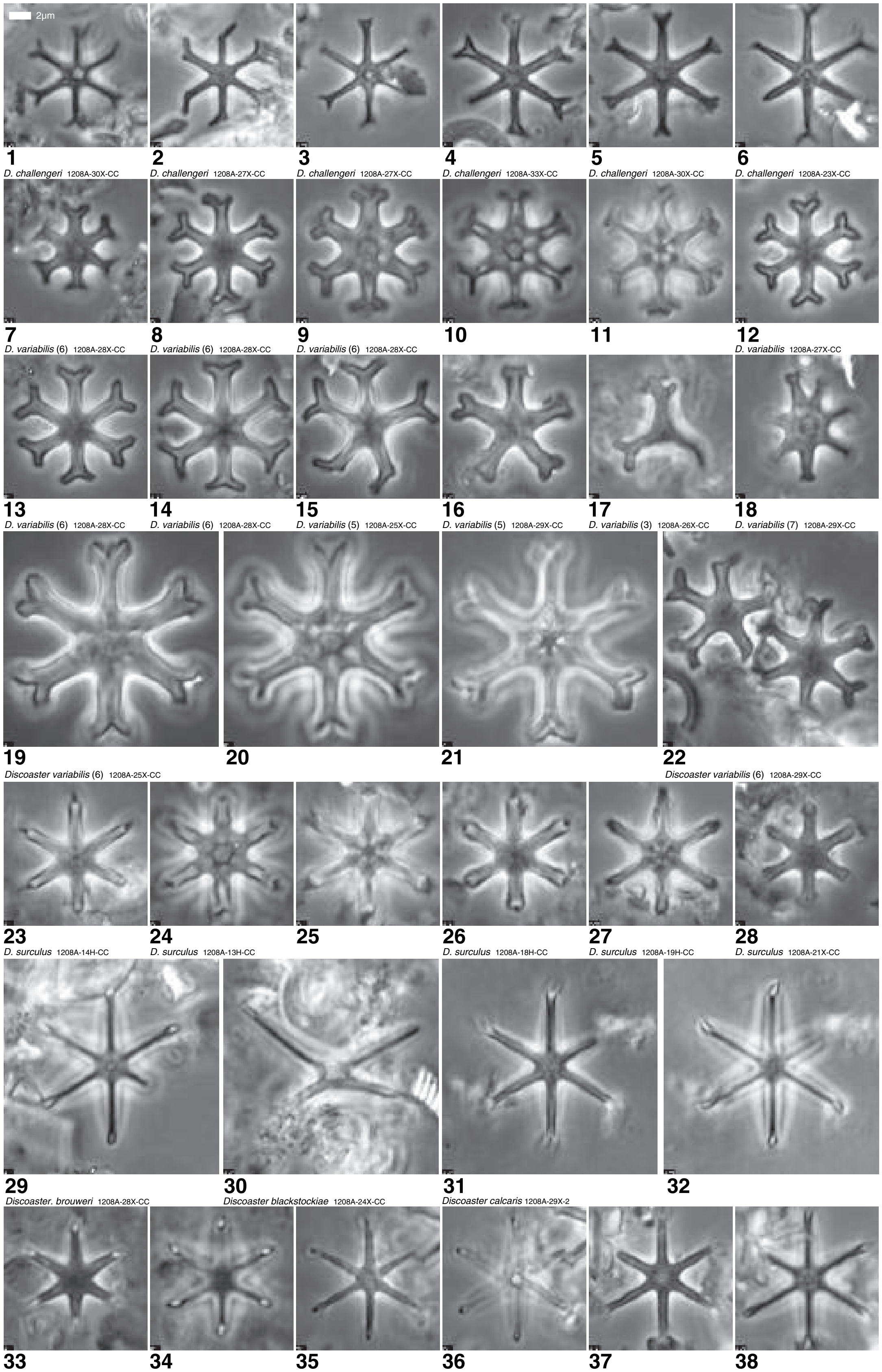

Plate P6. Discoasteraceae III. Taxonomic organization and concepts are generally comparable to those of Young and Bown (1997) and Young (1998). Images with black background are cross-polarized light images; those with light backgrounds are phase-contrast images. **1–6.** *Discoaster asymmetricus;* (1, 3–6) Sample 198-1208A-18H-CC, (2) Sample 198-1208A-21X-CC. **7–10.** *Discoaster tamalis;* (7, 9) Sample 198-1208A-15H-CC, (8) Sample 198-1208A-16H-CC. **10.** *Discoaster ?blackstockiae* (Sample 198-1208A-21X-CC). **11, 12.** *Discoaster triradiatus;* (11) Sample 198-1208A-28X-CC, (12) Sample 198-1208A-24X-CC. **13–18.** *Discoaster bellus* (Sample 198-1208A-29X-CC). **19–23.** *Discoaster hamatus;* (19, 20, 22, 23) Sample 198-1208A-29X-CC, (21) Sample 198-1208A-30X-CC. **24–34.** *Discoaster berggrenii;* (24, 25) Sample 198-1208A-26X-CC, (26, 27) Sample 198-1208A-25X-CC, (28, 29, 33, 34) Sample 198-1208A-27X-CC, (30–32) Sample 198-1208A-27X-5. **35–41.** *Discoaster quinqueramus;* (35, 40, 41) Sample 198-1208A-26X-CC, (36, 37) Sample 198-1208A-29X-CC, (38, 39) Sample 198-1208A-25X-CC. (**Plate shown on next page.**)

Plate P6 (continued). (Caption shown on previous page.)

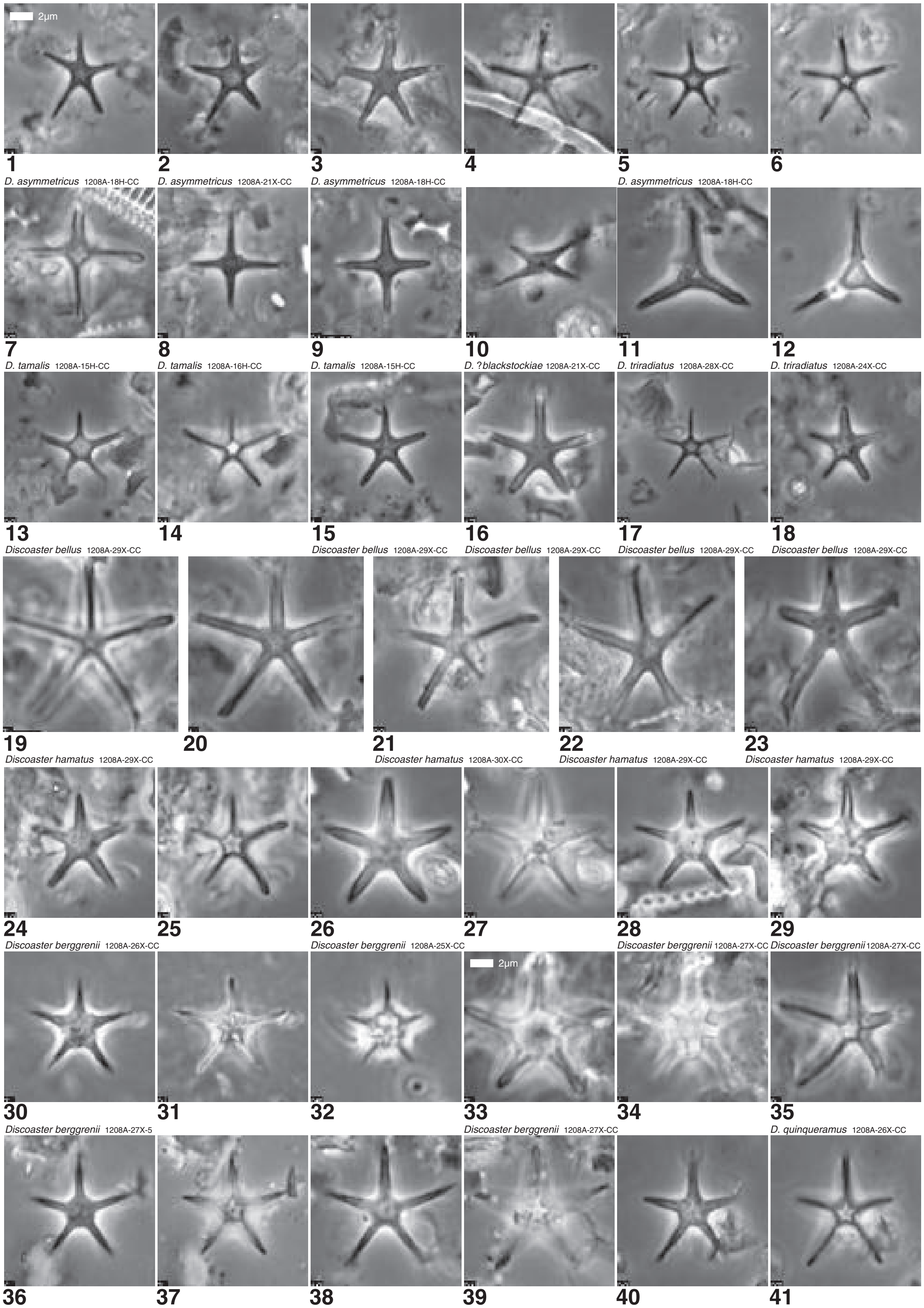

Plate P7. Discoasteraceae IV, Diatoms. Taxonomic organization and concepts are generally comparable to those of Young and Bown (1997) and Young (1998). Images with black background are cross-polarized light images; those with light backgrounds are phase-contrast images. **1–11.** *Discoaster pentaradiatus;* (1–4, 7–11) Sample 198-1208A-20H-CC, (5, 6) Sample 198-1208A-24X-CC. **12–17.** Sample 198-1208A-29X-CC. **18–23.** *Catinaster coalitus;* (18, 19) Sample 198-1208A-31X-2, (20–22) Sample 198-1208A-30X-CC, (23) Sample 198-1208A-30X-2. **24–29.** *Catinaster calyculus;* (24–27) Sample 198-1208A-30X-CC, (28, 29) Sample 198-1208A-30X-4. **30.** *Denticulopsis* sp. (Sample 198-1208A-19H-CC). **31.** *Actinoptychus* sp. (Sample 198-1208A-23X-CC). **32.** Diatom (Sample 198-1208A-30X-CC). **33, 34.** *Thalassiosira* sp.; (33) Sample 198-1208A-8H-CC, (34) Sample 198-1208A-4H-CC. **35.** *Cyclotella* sp. (Sample 198-1208A-1H-CC). **36.** *Discoaster* ?*variabilis* (Sample 198-1208A-28X-CC). **37, 38.** *Discoaster variabilis;* (37) Sample 198-1208A-28X-CC, (38) Sample 198-1208A-30X-CC. (**Plate shown on next page.**)

Plate P7 (continued). (Caption shown on previous page.)

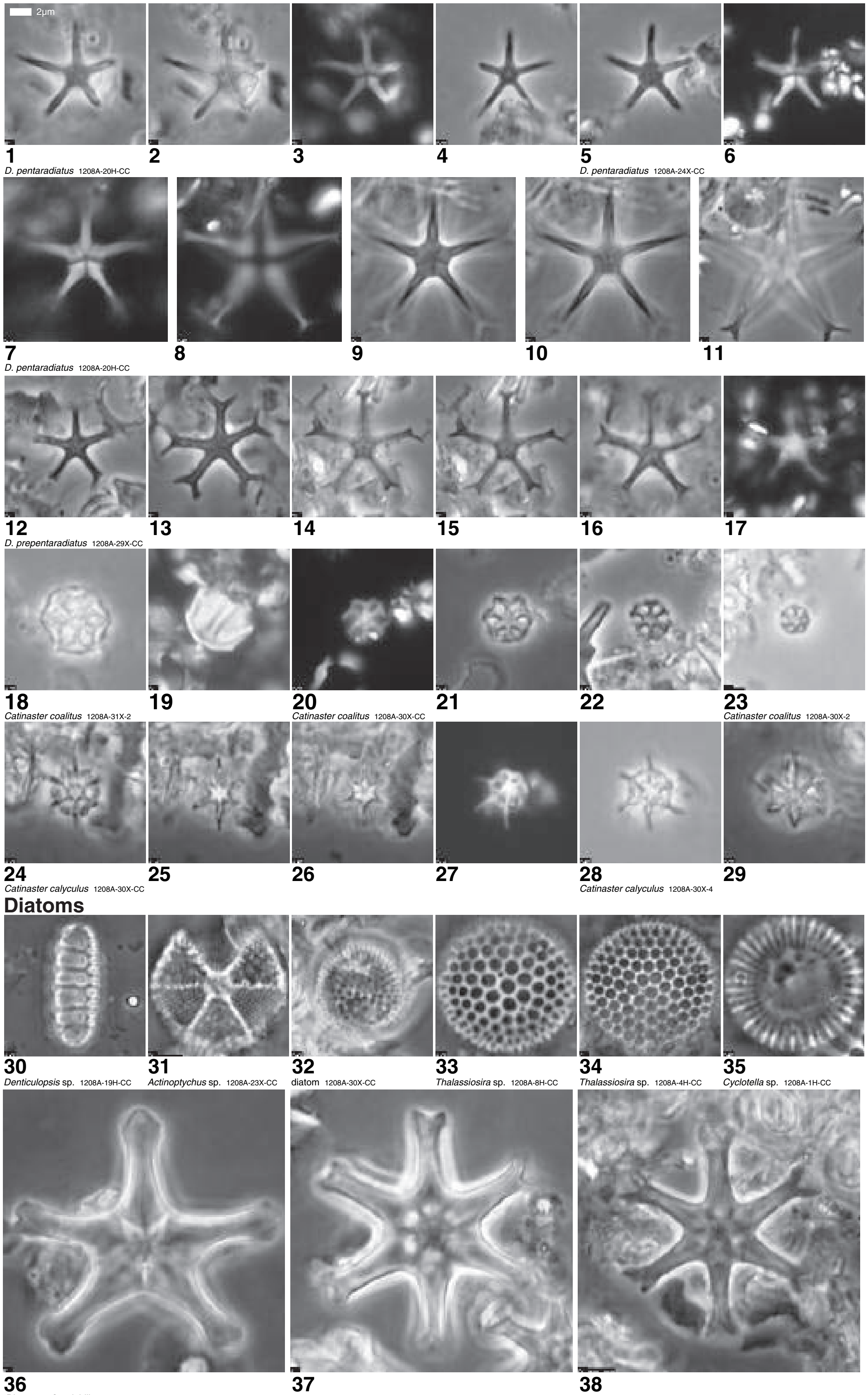

Plate P8. Noelaerhabdaceae, Coccolithaceae. Taxonomic organization and concepts are generally comparable to those of Young and Bown (1997) and Bown (2005). Images with black background are cross-polarized light images; those with light backgrounds are phase-contrast images. **1, 2.** *Chiphragmalithus barbatus* (Sample 198-1208A-35X-CC); (2) side view. **3.** *Isthmolithus recurvus* (Sample 198-1208A-36X-2, 30 cm). **4, 5.** *Neocrepidolithus grandiculus;* (4) Sample 198-1208A-36X-2, 99 cm, (5) Sample 198-1208A-36X-CC, 1.5 cm. **6.** *Toweius* cf. *T. callosus* (Sample 198-1208A-36X-2, 90 cm). **7.** *Cyclicargolithus abisectus* (Sample 198-1208A-36X-2, 3 cm). **8.** *Cyclicargolithus* cf. *C. floridanus* (Sample 198-1208A-36X-2, 3 cm). **9.** *Reticulofenestra bisecta* (8.5 µm) (Sample 198-1208A-35X-CC). **10, 11.** *Reticulofenestra stavensis;* (10) 10.6 µm (Sample 198-1208A-35X-CC), (11) Sample 198-1208A-36X-2, 40 cm. **12.** *Reticulofenestra umbilicus* (Sample 198-1208A-36X-2, 40 cm). **13.** *Bramletteius serraculoides* (Sample 198-1208A-35X-CC). **14.** *Campylosphaera* sp. (Sample 198-1208A-36X-2, 99 cm). **15.** *Chiasmolithus consuetus* (Sample 198-1208A-36X-CC, 2 cm). **16–18.** *Clausicoccus subdistichus;* (16) Sample 198-1208A-36X-CC, 8 cm, (17, 18) Sample 198-1208A-35X-CC. **19, 20.** *Coccolithus formosus* (Sample 198-1208A-35X-CC). **21, 22.** *Coccolithus pelagicus* (Sample 198-1208A-35X-CC). **23, 24.** *Ericsonia* cf. *E. robusta* (Sample 198-1208A-36X-CC, 12 cm). **15.** *Ericsonia robusta* (Sample 198-1208A-36X-CC, 5 cm). **26.** *Hayella situliformis* (Sample 198-1208A-36X-2, 3 cm). **27.** ?*Hughesius* sp. (Sample 198-1208A-36X-CC, 1.5 cm). **28–33.** *Calcidiscus pacificanus;* (28, 29) Sample 198-1208A-36X-CC, 1.5 cm, (30) Sample 198-1208A-36X-2, 30 cm, (31, 32) Sample 198-1208A-36X-2, 99 cm, (33) Sample 198-1208A-36X-2, 55 cm. **34.** *Markalius* sp. (Sample 198-1208A-36X-2, 55 cm). **35, 36.** Coccoliths (indeterminate) (Sample 198-1208A-35X-CC). **37, 38.** *Chiasmolithus consuetus* (Sample 198-1208A-36X-CC, 1.5 cm). **39.** *Reticulofenestra umbilicus* (18.5 µm) (Sample 198-1208A-35X-CC). **40.** *Reticulofenestra stavensis* (15.7 µm) (Sample 198-1208A-35X-CC). (**Plate shown on next page.**)

Plate P8 (continued). (Caption shown on previous page.)

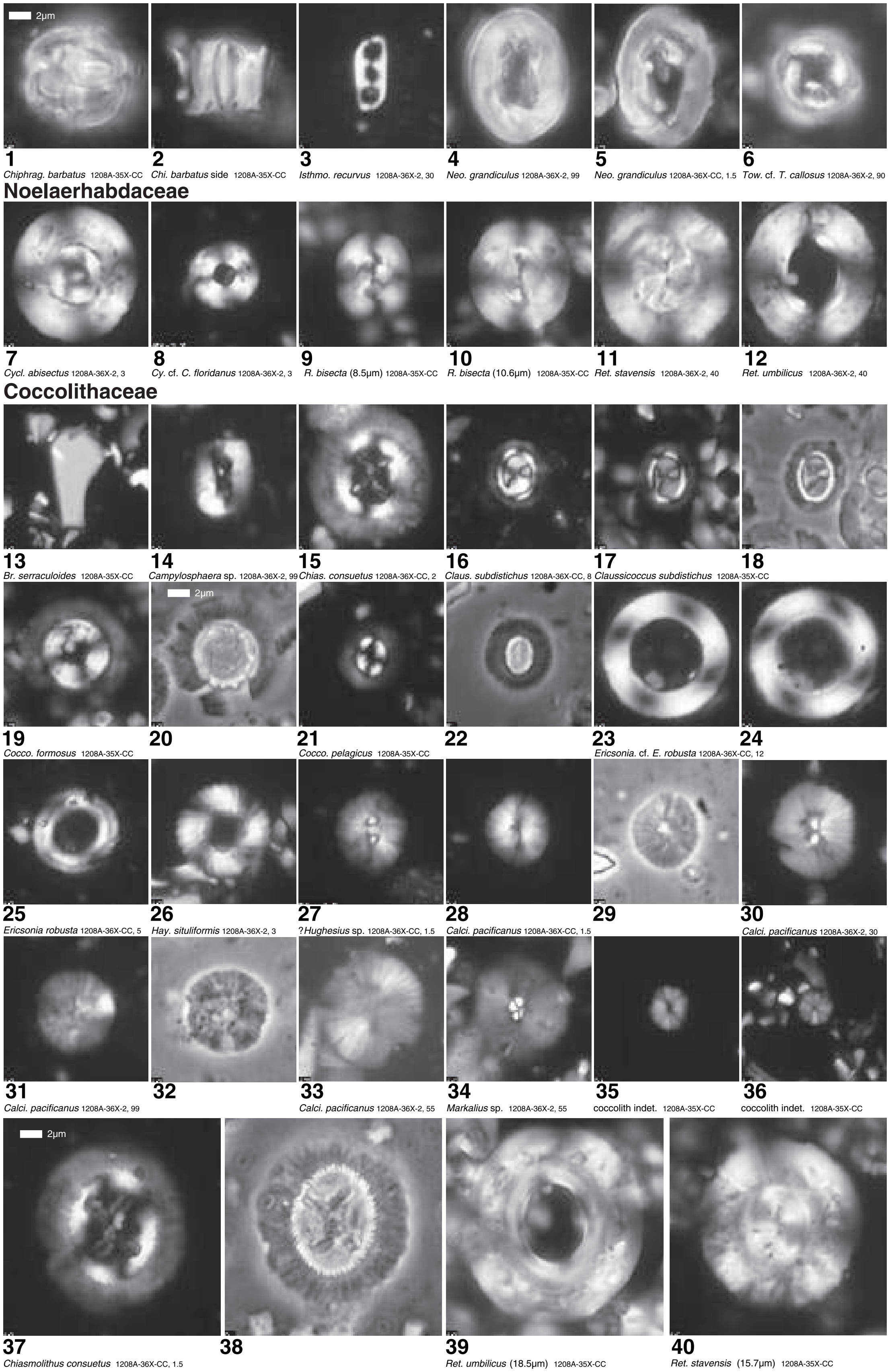

Plate P9. Sphenolithaceae. Taxonomic organization and concepts are generally comparable to those of Young and Bown (1997) and Bown (2005). Images with black background are cross-polarized light images; those with light backgrounds are phase-contrast images. **1–7.** *Sphenolithus arthurii* (Sample 198-1208A-36X-CC, 1.5 cm). **8–10.** *Sphenolithus ciperoensis* (Sample 198-1208A-35X-5, 10 cm). **11, 12.** *Sphenolithus predistentus* (Sample 198-1208A-35X-CC). **13, 14.** *Sphenolithus intercalaris* (Sample 198-1208A-35X-CC). **15–17.** *Sphenolithus conspicuus* (Sample 198-1208A-36X-2, 99 cm). **18.** *Sphenolithus moriformis* (Sample 198-1208A-35X-CC). **19, 20.** *Sphenolithus pseudoradians* (Sample 198-1208A-36X-2, 3 cm). **21, 22.** *Sphenolithus radians* (Sample 198-1208A-36X-2, 99 cm). **23–39.** *Sphenolithus villae;* (23, 24) Sample 198-1208A-36X-CC, 2 cm, (25–36) Sample 198-1208A-36X-2, 99 cm, (37–39) Sample 198-1208A-36X-CC, 1.5 cm. **40–46.** *Sphenolithus* cf. *S. delphix* (Sample 198-1208A-36X-2, 99 cm). **47, 48.** *Sphenolithus* cf. *S. spiniger* (Sample 198-1208A-36X-2, 99 cm). (**Plate shown on next page.**)

Plate P9 (continued). (Caption shown on previous page.)

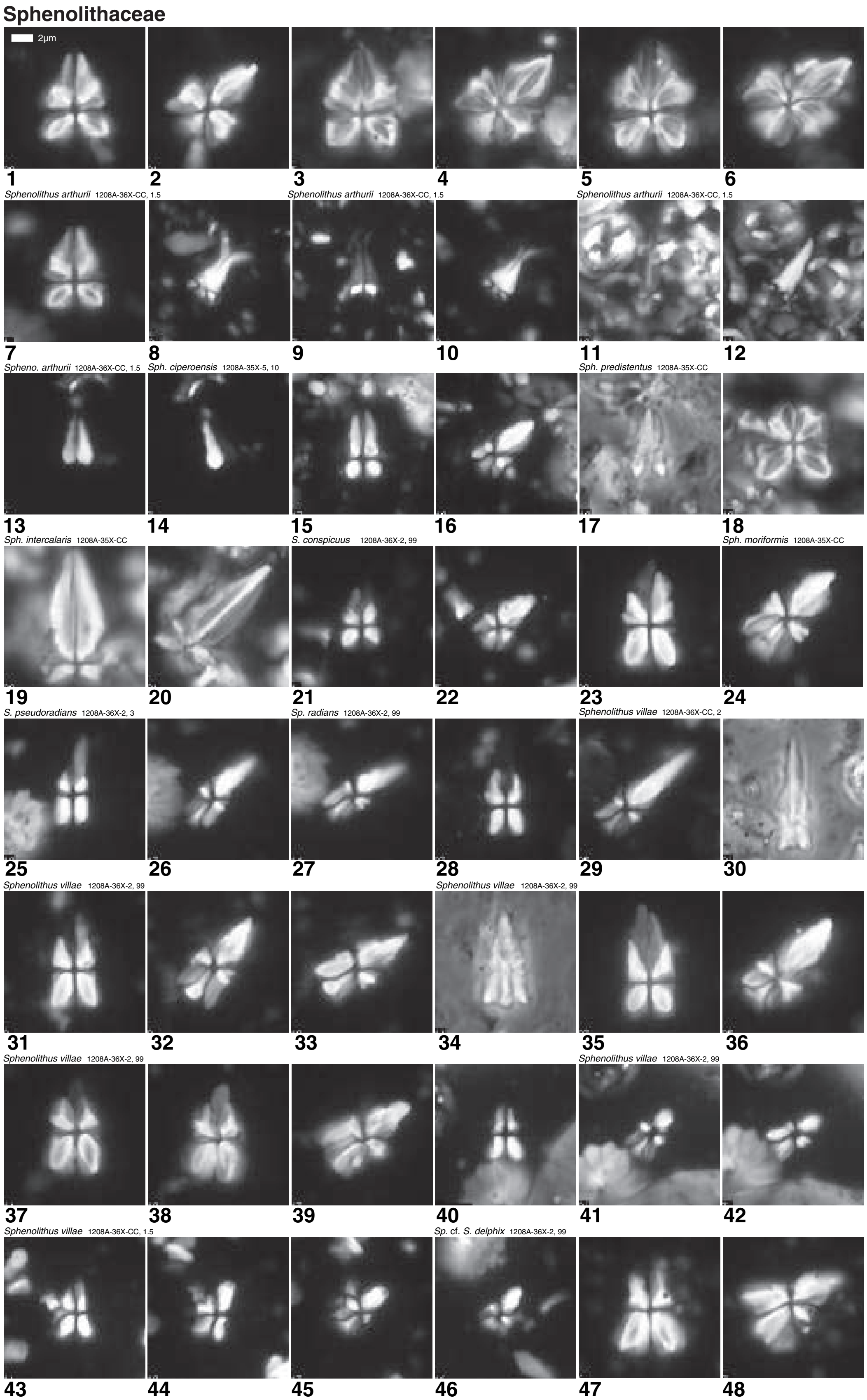

Plate P10. Discoasteraceae V. Taxonomic organization and concepts are generally comparable to those of Young and Bown (1997) and Bown (2005). Images with black background are cross-polarized light images; those with light backgrounds are phase-contrast images. **1, 2.** *Discoaster araneus;* (1) Sample 198-1208A-36X-CC, 8 cm, (2) Sample 198-1208A-36X-CC, 2 cm. **3.** *Discoaster* cf. *D. araneus* (Sample 198-1208A-36X-CC, 12 cm). **4, 5.** *Discoaster barbadiensis* (Sample 198-1208A-36X-CC, 1.5 cm). **6.** *Discoaster binodosus* (Sample 198-1208A-36X-CC, 1.5 cm). **7–12, 21, 28.** *Discoaster diastypus;* (7, 8) Sample 198-1208A-36X-2, 99 cm, (9–12, 21, 28) Sample 198-1208A-36X-CC, 1.5 cm. **13, 14.** *Discoaster lenticularis;* (13) Sample 198-1208A-36X-CC, 4 cm, (14) Sample 198-1208A-36X-CC, 12 cm. **15, 16.** *Discoaster mahmoudii* (Sample 198-1208A-36X-CC, 4 cm). **17.** *Discoaster mediosus* (Sample 198-1208A-36X-CC, 4 cm). **18.** *Discoaster mohleri* (Sample 198-1208A-36X-CC, 12 cm). **19, 20, 24–27.** *Discoaster* cf. *D. araneus;* (19, 24–26) Sample 198-1208A-36X-CC, 12 cm, (20) Sample 198-1208A-36X-CC, 14 cm, (27) Sample 198-1208A-36X-CC, 4 cm. **22.** *Discoaster lodoensis* (Sample 198-1208A-36X-2, 55 cm). **23.** *Discoaster tanii* (Sample 198-1208A-35X-CC). **29, 30.** *Discoaster multiradiatus* (Sample 198-1208A-36X-CC, 1.5 cm). **31.** *Discoaster mediosus* (Sample 198-1208A-36X-CC, 4 cm). (**Plate shown on next page.**)

Plate P10 (continued). (Caption shown on previous page.)

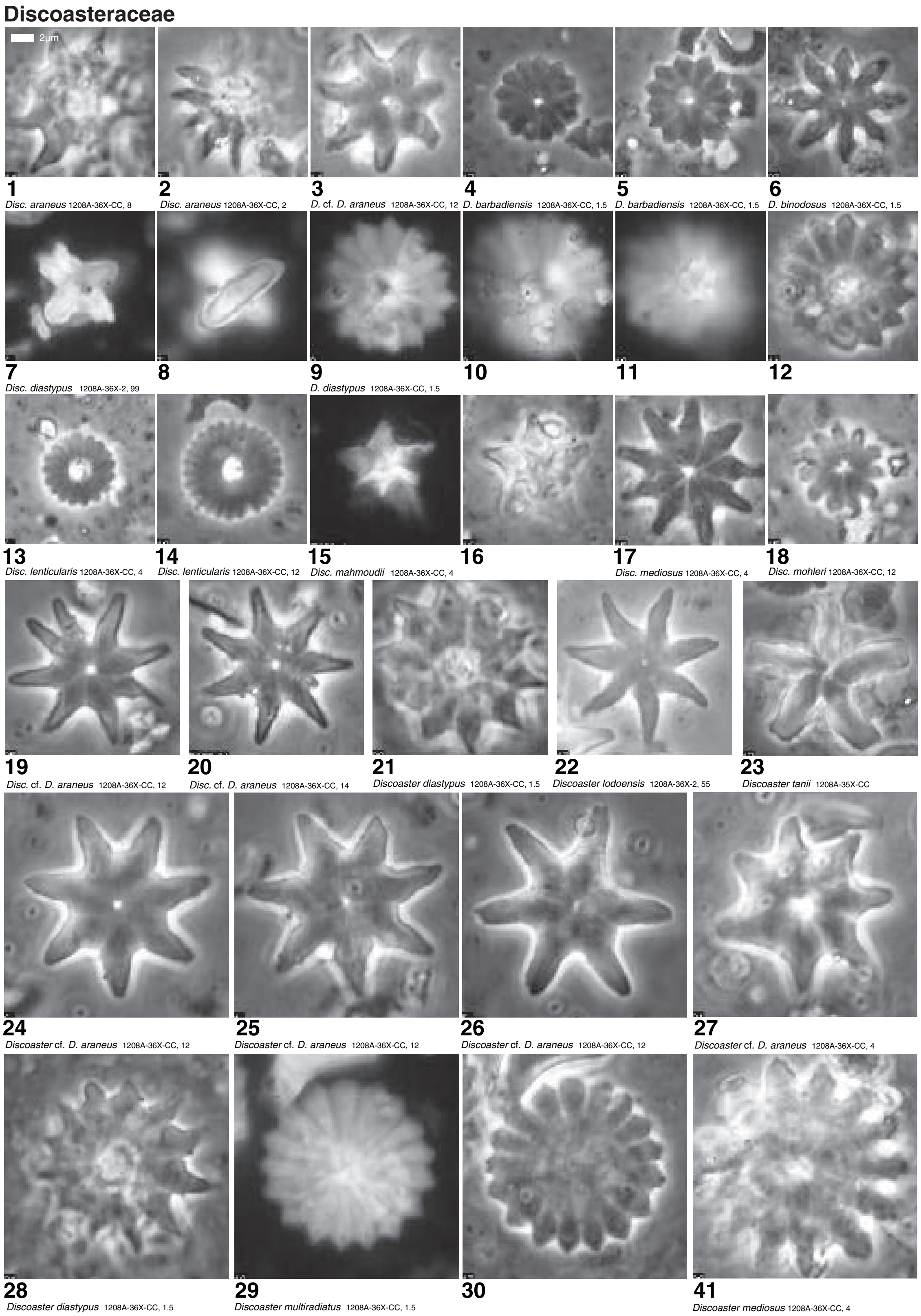

Plate P11. *Rhomboaster, Tribrachiatus.* Taxonomic organization and concepts are generally comparable to those of Young and Bown (1997) and Bown (2005). Images with black background are cross-polarized light images; those with light backgrounds are phase-contrast images. **1–12.** *Rhomboaster cuspis;* (1–5, 7–9) Sample 198-1208A-36X-CC, 4 cm, (6, 10–12) Sample 198-1208A-36X-CC, 5 cm. **13–23, 25–27.** *Rhomboaster bramlettei* (Sample 198-1208A-36X-CC, 4 cm); (22, 23) side view. **24.** *Rhomboaster bramlettei-spineus* (Sample 198-1208A-36X-CC, 4 cm). **28, 33.** *Tribrachiatus orthostylus;* (28) Sample 198-1208A-36X-CC, 1.5 cm, (33) Sample 198-1208A-36X-CC, 4 cm. **29–32, 34–36.** *Tribrachiatus contortus;* (29–32) Sample 198-1208A-36X-CC, 5 cm, (34, 35) Sample 198-1208A-36X-CC, 4 cm, (36) Sample 198-1208A-36X-CC, 2 cm. **37–39.** *Tribrachiatus digitalis* (Sample 198-1208A-36X-CC, 8 cm). (**Plate shown on next page.**)

Plate P11 (continued). (Caption shown on previous page.)

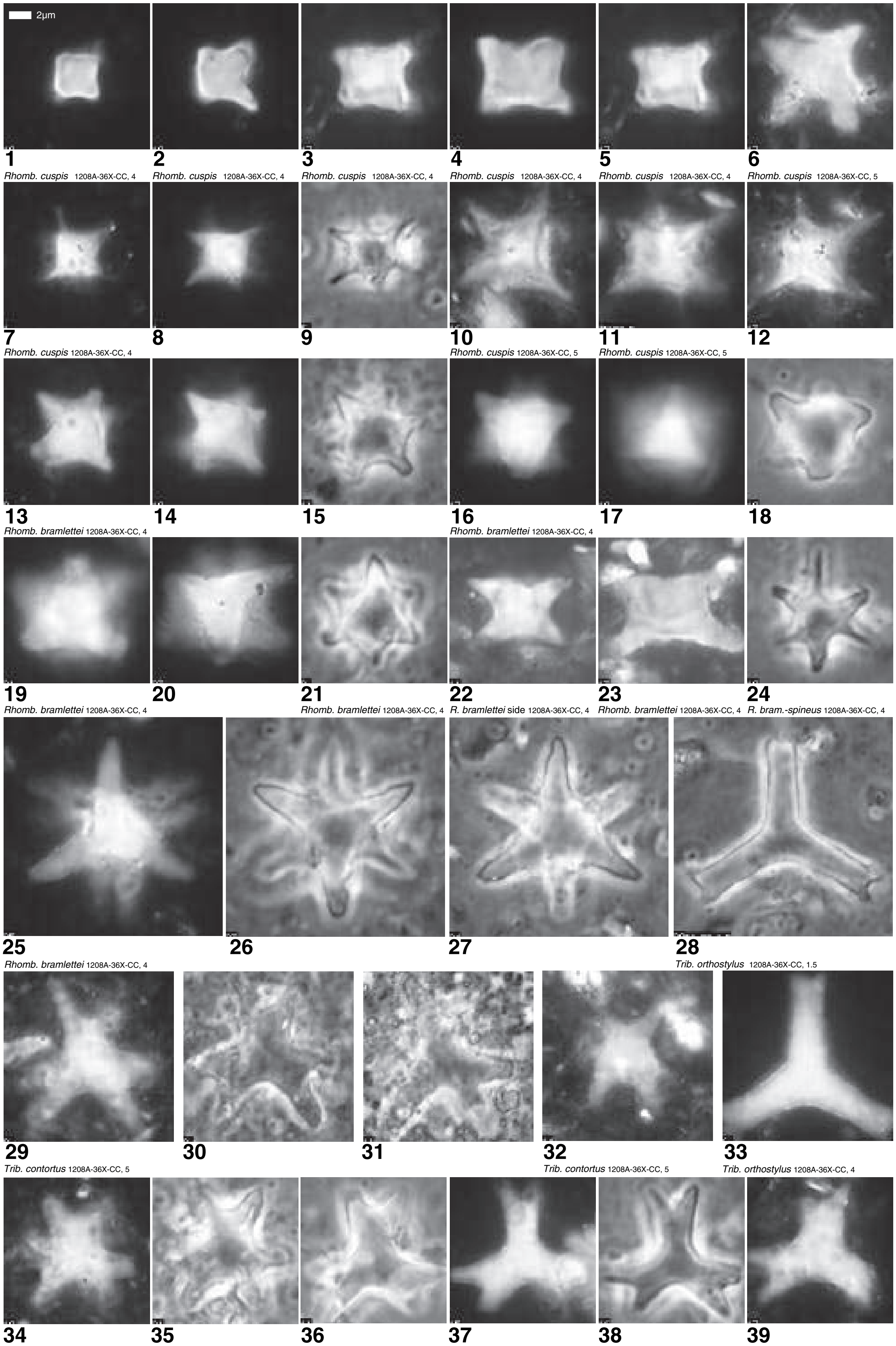

Plate P12. Fasciculithaceae. Taxonomic organization and concepts are generally comparable to those of Young and Bown (1997) and Bown (2005). Images with black background are cross-polarized light images; those with light backgrounds are phase-contrast images. **1, 2.** *Fasciculithus alanii* (Sample 198-1208A-36X-CC, 12 cm). **3.** *Fasciculithus aubertae* (Sample 198-1208A-36X-CC, 12 cm). **4–7.** *Fasciculithus bobii;* (4, 5) Sample 198-1208A-36X-CC, 14 cm, (6, 7) Sample 198-1208A-36X-CC, 12 cm. **8, 9.** *Fasciculithus tympaniformis;* (8) Sample 198-1208A-36X-CC, 8 cm, (9) Sample 198-1208A-36X-CC, 12 cm. **10–12, 28–33.** *Fasciculithus tonii;* (10–12, 28–30) Sample 198-1208A-36X-CC, 12 cm, (31–33) Sample 198-1208A-36X-CC, 8 cm. **13–16.** *Fasciculithus sidereus* (Sample 198-1208A-36X-CC, 8 cm). **17, 18.** Calcisphere; (17) Sample 198-1208A-36X-CC, 1.5 cm, (18) Sample 198-1208A-36X-2, 99 cm. **19–24.** *Fasciculithus fenestrellatus;* (19, 20) Sample 198-1208A-36X-CC, 8 cm, (21–24) Sample 198-1208A-36X-CC, 12 cm. **25–27.** F*asciculithus* sp. 1 (Sample 198-1208A-36X-CC, 8 cm). (**Plate shown on next page.**)

Plate P12 (continued). (Caption shown on previous page.)

Fasciculithaceae